The Aeronautical Journal (2022), **126**, pp. 59–91
doi:10.1017/aer.2021.92

SURVEY PAPER

NASA concept vehicles and the engineering of advanced air mobility aircraft

W. Johnson and C. Silva

National Aeronautics and Space Administration, Ames Research Center, Moffett Field, California, USA
E-mail: wayne.johnson@nasa.gov

Received: 12 July 2021; **Revised:** 21 September 2021; **Accepted:** 23 September 2021

Keywords: eVTOL; Rotorcraft; Design; Advanced Air Mobility; Urban Air Mobility

Abstract

NASA is conducting investigations in Advanced Air Mobility (AAM) aircraft and operations. AAM missions are characterised by ranges below 300 nm, including rural and urban operations, passenger carrying as well as cargo delivery. Urban Air Mobility (UAM) is a subset of AAM and is the segment that is projected to have the most economic benefit and be the most difficult to develop. The NASA Revolutionary Vertical Lift Technology project is developing UAM VTOL aircraft designs that can be used to focus and guide research activities in support of aircraft development for emerging aviation markets. These NASA concept vehicles encompass relevant UAM features and technologies, including propulsion architectures, highly efficient yet quiet rotors, and aircraft aerodynamic performance and interactions. The configurations adopted are generic, intentionally different in appearance and design detail from prominent industry arrangements. Already these UAM concept aircraft have been used in numerous engineering investigations, including work on meeting safety requirements, achieving good handling qualities, and reducing noise below helicopter certification levels. Focusing on the concept vehicles, observations are made regarding the engineering of Advanced Air Mobility aircraft.

Nomenclature

AAM	Advanced Air Mobility
AARON	AeroAcoustic ROtor Noise
AGL	above ground level
ANOPP2	Aircraft NOise Prediction Program 2
ATR	average temperature response
CAMRAD	Comprehensive Analytical Model of Rotorcraft Aerodynamics and Dynamics
CFD	computational fluid dynamic
CFR	code of federal regulations
CHARM	Comprehensive Hierarchical Aeromechanics Rotorcraft Model
dB	decibel, unit of sound intensity
DEP	distributed electric propulsion
DGW	design gross weight
DPFC	distributed propulsion and flight control
DRB	disturbance rejection bandwidth
EPNL	effective perceived noise level
ETS	emissions trading scheme
ESC	engine speed control
FHA	functional hazard analysis
FMECA	failure mode, effects, and criticality analysis
FTA	fault tree analysis

HECTR	high-efficiency civil tilt rotor
ISA	international standard atmosphere
MCP	maximum continuous power
MRP	maximum rated power (typically 10 min)
NASA	National Aeronautics and Space Administration
NDARC	NASA Design and Analysis of Rotorcraft
NOTAR	NO TAil Rotor
ODM	on-demand mobility
OEI	one engine inoperative
OGE	out of ground effect
QSMR	quiet single main rotor
RCOTools	Rotorcraft Optimisation Tools
RPM	revolutions per minute
RVLT	Revolutionary Vertical Lift Technology
SF	size factor
TRL	technology readiness level
UAM	Urban Air Mobility
VTOL	vertical take-off and landing
XDSM	eXtensible Design Structure Matrix

Symbols

A	rotor disk area, πR^2
A_{blade}	total blade planform area
C	charge capacity
C_T	rotor thrust coefficient, $T/\rho A V_{tip}^2$
C_W	aircraft weight coefficient, $W/\rho A V_{tip}^2$
D	rotor diameter, $2R$; drag
DL	disk loading, GW divided by total rotor disk area
FM	aircraft or rotor figure of merit
GW	gross weight (WO + payload + fuel)
I	current, $I = xC$
L	rotor lift
L/D_e	aircraft effective lift-to-drag ratio, WV/P
L/D_e	rotor effective lift-to-drag ratio, $LV/(P_o + P_i)$
P	power
P_o	profile power
P_i	induced power
R	rotor blade radius; range
T	rotor thrust
V	speed
V_{be}	best endurance speed (maximum 1/fuelflow)
V_{br}	best range speed (99% high side maximum V/fuelflow)
V_{cruise}	cruise speed
V_y	speed for best rate of climb
V_{tip}	rotor tip speed, ΩR
V_{H}	speed at maximum continuous power
W	weight
WE	aircraft empty weight
WO	operating weight (WE + fixed useful load)
x	current (capacity per hour)
ρ	air density
σ	rotor solidity, A_{blade}/A
Ω	rotor angular rotation speed

https://doi.org/10.1017/aer.2021.92 Published online by Cambridge University Press

1.0 Introduction

There is a dream growing now in the aviation community of providing air mobility as an alternative for everyday transportation requirements, described variously as On Demand Mobility (ODM), Urban Air Mobility (UAM), Air Taxi Operations or Advanced Air Mobility (AAM).

The invention of a practical aircraft for vertical take-off and landing — the helicopter — was largely accomplished by the end of the 1940s. Invention required solving the problems of flight: effective control (including rotor collective and cyclic), lightweight power (eventually turboshaft engines) and efficient structures (beginning with articulated and teetering blades). After invention, development turned to dealing with stability, high vibration and excessive noise, and then decades have been devoted to finding an aircraft that will combine greater speed and cruise efficiency with good hover and VTOL capability. AAM operations in urban areas are generally acknowledged to require VTOL capability [1–2], so achieving the dream will require new solutions to these old problems of rotorcraft, enabled by technology advances in noise, structures, automation and control, propulsion and energy generation-storage-utilisation, manufacturing and tools for VTOL aircraft design and analysis.

NASA is conducting research and investigations in Advanced Air Mobility (AAM) aircraft and operations. AAM missions are characterised by ranges below 300 nm, including rural and urban operations, passenger carrying as well as cargo delivery. Such vehicles will require increased automation and innovative propulsion systems, likely electric or hybrid-electric propulsion. Urban Air Mobility (UAM) is a subset of AAM and is the segment that is projected to have the most economic benefit and be the most difficult to develop. UAM requires an advanced urban-capable vehicle and an airspace system to handle high-density operations.

The NASA Revolutionary Vertical Lift Technology (RVLT) project is developing UAM VTOL aircraft designs [2–10] that can be used to focus and guide research activities in support of aircraft development for emerging aviation markets. These NASA concept vehicles encompass relevant UAM features and technologies, including propulsion architectures (distributed electric, hybrid, turboshaft, diesel), highly efficient yet quiet rotors and aircraft aerodynamic performance and interactions. The configurations adopted are generic, intentionally different in appearance and design detail from prominent industry arrangements, while capturing many of the essential technology features. The purpose of the NASA concept vehicles is to provide specific configurations for communication of NASA's Urban Air Mobility research, for support of design and analysis tool development, for technology trade studies and sizing excursions, and for modeling operational scenarios. These aircraft are common configurations for studies in acoustics, flight dynamics, propulsion safety and reliability, crashworthiness, and other disciplines, both within and external to NASA. Data on the NASA concept vehicles will be widely shared and fully documented; they have realistic performance and are based on a realistic set of design compromises. NASA has no plan to build or fly these concepts.

The NASA concept vehicles were developed in several phases: reduced-emission rotorcraft concepts [3]; concept vehicles for operations at several aircraft sizes (number of passengers and range, [4]); and vehicles for a UAM design mission [6, 8–9]. The UAM design mission was identified as carrying six passengers over a 75 nm range (with 10 kt headwind), and 20 min cruise reserve [5]. The principal concept vehicles developed for this mission are quadrotor, side-by-side helicopter, lift+cruise, single main rotor and tiltwing configurations. Additional concept vehicles are currently being examined, including a tiltrotor aircraft and a tilting-ducted-fan configuration. These UAM concept aircraft have been used already in numerous engineering investigations.

This paper summarises the results of these recent NASA investigations. The software tool suite used is outlined, and the concept aircraft developed are described. Observations about the design trade-offs and key design decisions are discussed. The viewpoint presented is that of the design group in the NASA RVLT project.

https://doi.org/10.1017/aer.2021.92 Published online by Cambridge University Press

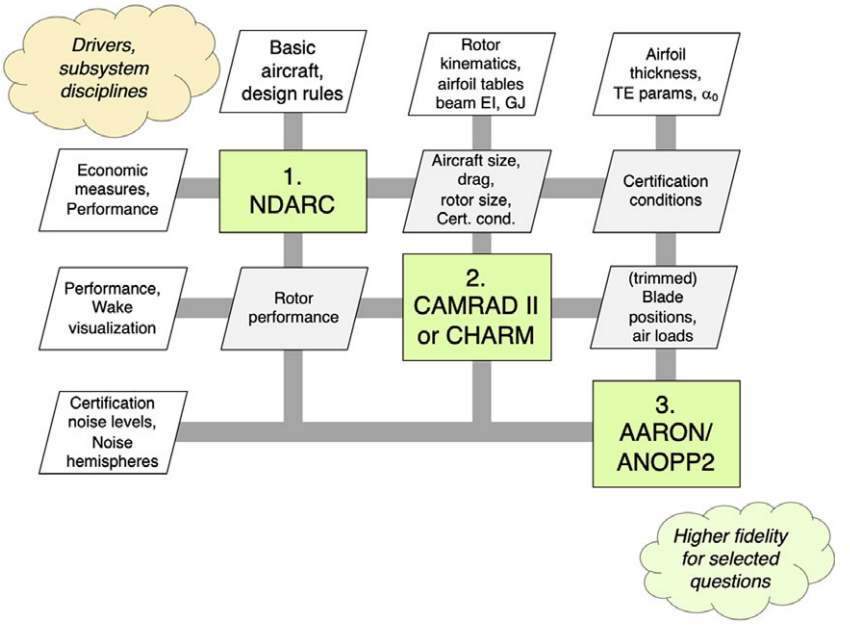

Figure 1. *Diagram of the tools and workflow as the central part of a conceptual design process.*

2.0 Design and analysis tools

The process and tools for development of the NASA concept vehicles are described in Reference 10. Figure 1 illustrates the central tools in terms of an eXtensible Design Structure Matrix (XDSM) diagram. The primary tools for performing physical calculations are on the diagonal of the matrix as green rectangles, interconnections are grey lines and data entities are parallelograms. Data transfer and inter-tool design process are managed by scripts written in Python. The clouds at either end of the diagonal indicate that this toolchain can be integrated as part of a larger process. Overall inputs are in the white parallelograms at the top, and overall outputs are white parallelograms at the left. Guided design space exploration such as parameter sweeps, optimisation drivers, vehicle type comparison may be implemented in the upper-left, orange-coloured cloud, along with other subsystem design (e.g. propulsion, flight control). On the lower-right, the green-coloured cloud indicates where vehicle and subsystem design of higher fidelity would be added in order to verify earlier conceptual design assumptions, or capture phenomena that are inadequately addressed in earlier steps of the conceptual design process (e.g. a set of coupled CFD download and aerodynamic interaction calculations for key sizing conditions).

2.1 NDARC

Primary sizing and performance analysis of the aircraft is performed by NASA Design and Analysis of Rotorcraft (NDARC, [11–12]). NDARC has a modular architecture, facilitating its application to new aircraft and propulsion types, including non-traditional propulsion systems. Aircraft are represented as a collection of components, with surrogate or semi-analytic models for performance and weight of each component. NDARC performs fixed-point iteration to find the vehicle size based on specified sizing rules, missions and flight conditions. The most complete description of the concept aircraft is encapsulated in NDARC output files. NDARC is capable of assessing the impact of advanced technology and design choices. NDARC calculates economic measures, such as productivity, flyaway cost and operating cost for the concept aircraft. For a sized aircraft, NDARC calculates the weights and speeds to fly the required operations, such as noise metric conditions, as these are vehicle-specific, and must consider nonlinearities and limits in the propulsion system, not just aerodynamic performance.

https://doi.org/10.1017/aer.2021.92 Published online by Cambridge University Press

Advanced technology is incorporated in NDARC models in terms of the surrogate models for rotor and engine/motor performance, battery weight and efficiency and technology factors for component weights. Often useful aircraft technologies (such as active flow control) must be integrated into the design, accounting for weight and power increments as well as performance and efficiency improvements.

2.2 CAMRAD II or CHARM

A comprehensive analysis code simultaneously solves the rotor dynamics and aerodynamics for a trimmed or transient flight condition. CAMRAD II was used in the optimisation of the rotor geometry for the aircraft sizing conditions, and to develop calibrated rotor performance models for NDARC; as well as to calculate rotor and hub loads for structural design, assess rotor and blade stability and whirl flutter, and provide rotor blade airloads for mid-fidelity acoustics calculations. NASA is not actively developing its own comprehensive analysis solution, rather is applying commercial software for this step in the process. Two commercial codes, CAMRAD II [13–14] and CHARM [15], are being integrated interchangeably into the toolchain. By using two codes, a robust application programming interface can be defined that will allow other comprehensive analysis codes to be integrated into the toolchain. Both CAMRAD II and CHARM have well-validated free wake modeling capability. For interacting rotors, a freely convecting wake is necessary to accurately predict performance, as well as blade-vortex-interaction airloads that are responsible for significant noise. For example, lift+cruise, quadrotor, and side-by-side aircraft have rotors that interact to varying degrees in various stages of flight. Similarly, for practical UAM rotors larger than a couple of feet in radius, elastic and kinematic motion should be considered to calculate the rotor trim and blade-vortex interactions. Blade airloads and velocities will in general depend on blade motion, induced velocity, and wake convection. Whether or not the aerodynamic model of a comprehensive analysis code is adequate for evaluating the noise sources, a comprehensive analysis model of the structure is required. Building a comprehensive analysis model is generally a necessary step in the development of a meaningful high-fidelity simulation, as vehicle trim, rotor trim and blade kinematic and elastic motion are usually computed by a comprehensive analysis, which is coupled to CFD airloads.

2.3 AARON/ANOPP2

In order to predict the acoustic metrics, a tool that predicts thickness, loading, and broadband noise, acoustic propagation and observer noise is necessary. The Aircraft NOise Prediction Program 2 (ANOPP2, [16–18]) and AeroAcoustic ROtor Noise (AARON) tools provide the acoustic calculations in the toolchain. AARON is the user code to perform rotorcraft calculations with ANOPP2. A Python script provides a simplified interface that is geared toward generating the certification noise and other typical rotorcraft calculations with a manageably small number of inputs. AARON/ANOPP2 calculates the loading noise with a compact loading model, using the blade section loading and motion as well as the aircraft operating condition from the comprehensive analysis. Consistently, thickness noise is calculated with a compact monopole model. An aerofoil self-noise model extended to rotating blades is used for broadband noise [18]. AARON/ANOPP2 can also calculate the loading and rotational noise from a higher-fidelity solution for the blade surface pressures and geometry, such as from CFD calculations.

2.4 RCOTools

Rotorcraft Optimisation Tools (RCOTools, [19]) is a set of Python libraries that serve as application wrappers for input/output and program execution of several tools. In this toolchain, RCOTools interfaces for NDARC and CAMRAD II/CHARM are used. The data connections depicted by grey lines in the XDSM diagrams of Fig. 1 are facilitated by RCOTools.

https://doi.org/10.1017/aer.2021.92 Published online by Cambridge University Press

2.5 Additional tools

Other tools are available to provide detailed models and data for the principal codes: engine models (NPSS [20]); handling qualities assessment (SIMPLI-FLYD [21]; and FlightCODE); structural design and analysis (IXGEN [22] and M4 Structures Studio [23]); geometry and layout (OpenVSP [24] for initial geometry; Rhino for final geometry); and high-fidelity aerodynamic loading (OVERFLOW [25] and FUN3D [26]).

2.6 Assessment of tools

A goal of the present tool suite development effort within NASA's RVLT project is to provide robust computational methods that facilitate design space exploration with varied problem definitions and with the ability to concurrently consider several different potential solutions. The development of the NASA concept vehicles has demonstrated that the computational tools available for rotorcraft aeromechanics analysis and design are generally applicable to VTOL AAM aircraft. In particular, the toolchain has been capable of quantitatively trading several relevant noise reduction technologies and design approaches for aircraft that can perform the Urban Air Mobility mission [10]. The calculations performed for these trades are quick enough to allow several simultaneous aircraft types to be evaluated by an individual designer or design team, with the calculations performed on workstation computers. The tools are practical, in terms of the amount of input required and the computation times [10].

3.0 Reduced-emission rotorcraft concepts

A prelude to the design of aircraft for UAM missions was an investigation of VTOL aircraft optimised for reduced emissions and acoustics [3]. Rotorcraft concepts were developed with the goal of producing less than 50% of the climate-impacting emissions of today's fielded technology. NDARC has two models for emissions [11]: the emissions trading scheme (ETS) of the European Union, which accounts for CO_2 only (the metric is kg CO_2 per mission); and the average temperature response (ATR), which captures long-time integrated effects of CO_2, H_2O, NO_x, O_3, CH_4, SO_4, soot and aviation induced cloudiness (the metric is nano-°C of warming per mission). For electric propulsion, the ETS method includes the CO_2 produced in generating the energy. For turboshaft propulsion, the ATR method uses an engine NO_x emission model.

Reduced-emission rotorcraft concepts were developed for three aircraft size classes:

a) Class A: 5 passengers plus pilot, 400 nm range; baseline single main rotor and tail rotor helicopter;

b) Class B: 24 passengers plus 3 crew, 500 nm range; baseline single main rotor and tail rotor helicopter;

c) Class C: 76 passengers plus 5 crew, 1,300 nm range; baseline conventional tiltrotor.

The baseline aircraft represent today's technology (TRL 9): un-faired hubs and aluminium structure for helicopters; fly-by-wire and fastened composites for tiltrotors; current technology turboshaft engines; crashworthy structures; and inclement weather operation.

Figure 2 shows the reduced-emission rotorcraft designs. The principal characteristics of the baseline and reduced-emission designs are given in Table 1. While several advanced aircraft types were considered (Fig. 2), Table 1 only presents the baseline and the best (lowest-emission) designs for each class. Advanced technologies (TRL 5+) considered include more attention to drag (faired hubs, landing gear), more composite structures (bonded instead of fastened), advanced drive systems materials and approaches, and advanced turboshafts for classes B and C. These technologies alone could not make the helicopters clean enough, with only about 20% reduction in emissions for class A, and

https://doi.org/10.1017/aer.2021.92 Published online by Cambridge University Press

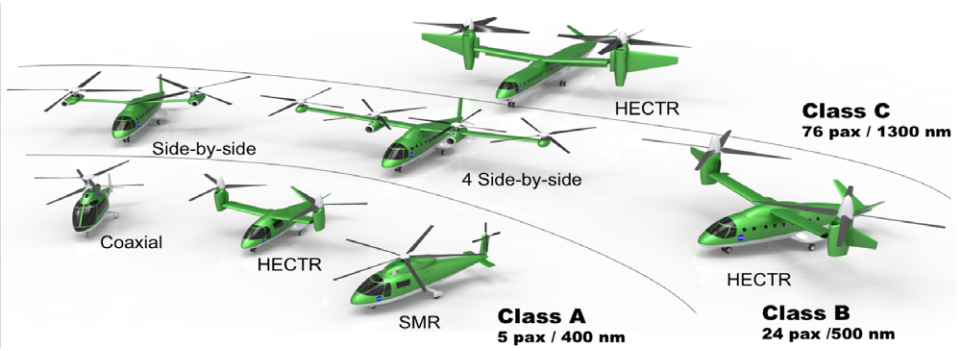

Figure 2. *Reduced-emission rotorcraft concepts: environmentally friendly aircraft designs [3].*

Table 1. Characteristics of reduced-emissions aircraft [3]

		Class A		Class B		Class C	
		Single Main-Rotor baseline	Coaxial low emission	Single Main-Rotor baseline	Side-by-Side low emission	Tiltrotor baseline	HECTR low emission
Payload	lb	1,000	1,000	5,280	5,280	16,500	16,500
Range	nm	400	400	500	500	1,300	1,300
Rotor radius	ft	15.2	13.7	29.6	23.2	27.8	26.5
Disk loading	lb/ft^2	8.0	8.0	9.0	6.0	20.0	15.7
Power	hp	1,070	766	9,829	3,300	31,586	23,722
DGW	lb	5,781	4,586	36,402	20,223	135,260	69,163
Empty weight	lb	3,597	2,694	23,942	11,906	90,248	40,729
Fuel burn	lb	855	594	5,732	2021	25,763	8,880
ETS	kg CO_2	1,637	1,141	10,897	3,835	46,222	16,287
ATR	nano°C	10.4	7.3	68	24	314	110
Emissions reduction	%		30%		65%		65%

35%–40% reduction for classes B and C. Considering more efficient aircraft types was necessary: coaxial helicopters, side-by-side helicopters and high-efficiency civil tiltrotors (HECTR). The HECTR design for class C achieved 70% reduction of emissions. The side-by-side helicopter (2 or 4 rotors) and the HECTR achieved 65% reduction of emissions for class B. The lack of an efficient small (<1,000 shp) turboshaft development meant that turboshaft-power designs for class A did not achieve the goal of 50% reduction: only achieved 20% reduction of emissions for the single main-rotor and tail-rotor helicopter, 30% reduction for the coaxial helicopter or tiltrotor (the tiltrotor does not get light enough to take advantage of its cruise efficiency).

Electrical propulsion concepts were examined for the smaller classes, considering very long-term goals for weights and efficiencies (currently below TRL 2). Battery-powered aircraft do not meet the goal, since besides increasing the vehicle weight, U.S. electric grid emissions are high. Emissions from fuel cells can be very low, even if the hydrogen is obtained from a methane source, although the weights are high.

This work on low-emission rotorcraft provided the foundation for exploring UAM designs: development of an integrated tool suite for the multidisciplinary design and optimisation of VTOL aircraft;

https://doi.org/10.1017/aer.2021.92 Published online by Cambridge University Press

Figure 3. *Concept aircraft: single-passenger quadrotor with electric propulsion, 15-passenger tiltwing with turboelectric propulsion, and 6-passenger side-by-side helicopter with hybrid [4].*

demonstration of alternative propulsion architectures in NDARC, including electric power; and quantification of the cruise efficiency of the side-by-side helicopter type.

4.0 Concept vehicles for air taxi operations

To begin the process of developing concept vehicles for air taxi operations, the range of aircraft attributes being considered by the design community was examined:

a) number of occupants (including pilot): 1, 2, 4, 6, 15, 30
b) un-refueled range: 50, 100, 200, 400, 800 nm (as multiples of 50 nm segments for this investigation)
c) market: air taxis, commuter scheduled, mass transit, airline
d) aircraft type: multicopter, side-by-side, tiltwing, tiltrotor, lift+cruise, vectored thrust, compound, helicopter
e) propulsion system: turboshaft, turbo-electric, electric, parallel hybrid, fuel cell, diesel

NASA developed three concept vehicles ([4], Fig. 3) that encompass many elements of this design space:

1) A single-passenger (250-lb payload), 50-nm range quadrotor with electric propulsion (with interconnect shaft between rotors), using flapping rotors and collective control; design excursions included rigid rotors, rotor speed control (fixed pitch blades) and reciprocating engines.
2) A six-passenger (1,200-lb payload), 200-nm range (four 50-nm trips) side-by-side helicopter with hybrid propulsion; excursions included turboshaft and electric propulsion.
3) A 15-passenger (3,000-lb payload), 400-nm range (eight 50-nm trips) tiltwing with turbo-electric propulsion, using four propellers with collective and cyclic control; design excursions included tail propellers for pitch and directional control.

The principal characteristics of these concept aircraft are given in Table 2.

The primary sizing mission consists of the following segments: (1) 2-min hover out-of-ground-effect (OGE) for takeoff; (2) fly 50 nm at best-range speed; (3) 2-min hover OGE for landing; (4) fuel/energy reserve minimum of 10% of mission or 20-min flight at best-endurance speed (V_{be}). All the segments are flown at atmospheric conditions of 5,000-ft altitude and ISA + 20°C temperature. Segments 1–3 are repeated for each 50 nm leg in the un-refueled range. Cruise is flown at best-range speed (V_{br}, 99% high side), unless the maximum speed is less than V_{br}. Reserve requirements are based on 14 CFR 91.151: 20-min at cruise speed for visual flight rules (VFR) rotorcraft. A second sizing mission has these segments flown at sea level and ISA + 20°C temperature.

All-weather operations are assumed, which has an impact on systems weight (including de-icing). For low aircraft noise, the design rotor tip speed is low compared to conventional helicopters: 450 ft/sec for

https://doi.org/10.1017/aer.2021.92 Published online by Cambridge University Press

Table 2. Characteristics of concept aircraft for initial air taxi mission [4]

Aircraft Propulsion		Quadrotor Electric	Side-by-Side Hybrid	Tiltwing Turbo-electric
Payload	lb	250	1,200	3,000
Range	nm	50	200	400
Rotor radius	ft	6.5	11.8	6.1
Disk load	lb/ft^2	2.5	4.5	30.0
$L/D_e = WV/P$		5.3	6.0	7.2
Power	hp	4x23	2x187 + 100*	4x731 + 4,730**
DGW	lb	1,325	3,950	14,039
Empty weight	lb	1,070	2,390	8,918
Structure	lb	394	1,050	3,495
Propulsion	lb	118	562	3,010
Battery	lb	286	103	450

*turboshaft & motor **motor & turboshaft

the quadrotor, 550 ft/sec for the larger aircraft. (In general, reducing the design hover tip speed increases the size of the aircraft; the consequences of weight growth are less for a small aircraft, so a lower tip speed can be used for the quadrotor.) Maximum speed (from power available at 90% MCP) is fallout (not specified), with installed power determined by takeoff conditions.

4.1 Battery technology

Light and efficient batteries are crucial to producing good designs for electric aircraft. The electric designs for these aircraft assume an installed, usable battery specific energy of 400 Wh/kg (pack). Internal resistance reduces battery efficiency at high discharge rates, so typical Li-ion battery discharge characteristics are used to calculate the efficiency. Margins for maximum charge and discharge are established to prolong battery life (in terms of discharge-charge cycles): charge to within 5%–10% of full capacity, discharge to 15%–20% capacity. Current delivery limits for cells are specified as a C-rate (capacity/hr). Even with a high maximum burst discharge capability (high maximum power), discharge currents in today's high-specific-energy Li-ion cells must be limited to 2–3C for good battery life. The installed specific energy is reduced by packaging and conditioning requirements, including thermal management systems. For the electric propulsion variants of the three configurations, design excursions of range and battery technology were generated to quantify the impact on aircraft weight, power, and feasibility. Specific weight, the crucial aspect of battery technology for aircraft design, was considered from 400 Wh/kg down to 150 Wh/kg (values for pack, not cell). Below about 300 Wh/kg, the range capability was reduced while the aircraft weight increased. Having established these trends, a high level of battery technology had to be assumed for the UAM concept vehicles to ensure that the designs would meet the mission requirements.

5.0 Vehicles for the UAM mission

Following the initial air taxi vehicle study, which explored vehicle technology themes using aircraft of various sizes designed for several candidate missions, RVLT performed a focused study to better understand a particular urban air mobility market. A design mission was developed accounting for the existing geography, population patterns, infrastructure and weather in 28 markets across the United States [5]. The resulting mission is to carry six passengers (including the pilot, if not autonomous; 1,200 lb payload) on two 37.5-nm flights (total 75-nm range without recharging or refueling), with a 20 min reserve (Fig. 4). Takeoff altitude is 6,000-ft (ISA), and cruise is at best range speed, 4,000-ft above ground level (AGL). This mission is intended to be used as a sizing requirement. The actual

https://doi.org/10.1017/aer.2021.92 Published online by Cambridge University Press

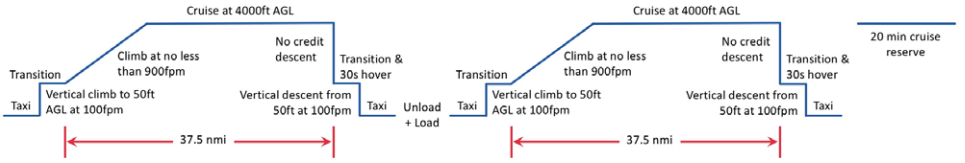

Figure 4. *UAM sizing mission profile [5].*

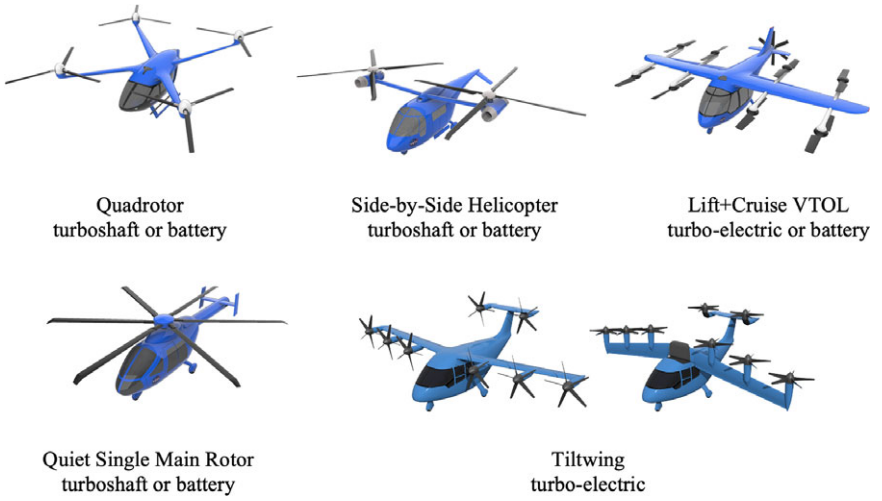

Figure 5. *UAM aircraft designs: six occupants (1,200 lb), 75 nm range [6, 8–9].*

operational missions flown by the aircraft will be different, driven by economics, air traffic, and other aspects of a particular flight.

In order to quantify the tradeoffs and performance targets necessary for practical implementation of the UAM vision, NASA concept vehicles were designed to perform this mission [6, 8–9]. A range of aircraft types and propulsion system architectures were considered (Fig. 5): quadrotor aircraft, with turboshaft and electric propulsion; side-by-side aircraft, with turboshaft and electric propulsion; lift+cruise aircraft with electric and turbo-electric propulsion; a quiet single-main rotor helicopter with turboshaft and electric propulsion; and a tiltwing aircraft with turbo-electric propulsion.

Certain technologies and attributes that are expected to be included in a new-start aircraft have been included in the models for all of the concept vehicles. These features include muffling of the engine and drive system to reduce noise to a level lower than that of the rotor system, with associated weight and performance penalties. Systems weights include instrumented flight rules-capable avionics, cockpit controls, and fly-by-wire flight controls; these weights serve as the initial budget for an autonomous flight control system. Vibration mitigation weights have been included for each of the aircraft. Furnishings weights include crashworthy seats, sound dampening, and environmental control systems. The airframe and rotor structures use technology factors calibrated to composite rotorcraft with crashworthiness considerations. The turboshaft engines represent state-of-the-art turboshafts, which at this scale are relatively fuel-thirsty and have not had much technology insertion for many decades. Further discussion of technologies for the concept aircraft may be found in [7].

Consistent technology assumptions were made to size the vehicles:

a) Battery pack modeled as Li-Ion (TRL 1): installed, usable specific energy 400 Wh/kg (well beyond state-of-the-art); maximum mission current 4C, emergency 14C (high end state-of-the-art); wiring and accessory electric systems as fractions of motor weight (TRL 3)

b) Structures (TRL 3+): composite VTOL structures, very lightweight booms

https://doi.org/10.1017/aer.2021.92 Published online by Cambridge University Press

c) Aerodynamics (TRL 5+): passive rotor and airframe lift/drag

d) Propulsion (TRL 5+): high torque/weight electric motors; high torque/weight transmissions

e) Systems (TRL 5+): equipment for instrument flight rules (IFR) operations (hence autonomy possible without additional weight); environmental control systems, insulation, seating

All aircraft (five aircraft types so far, two propulsion architectures for most, plus numerous excursions) were designed to the same mission. The principal characteristics of the designs are given in Table 3. Figure 6 shows the breakdown of the weight empty. For each design, the payload is 1,200 lb and the fuel for turboshaft propulsion is 150–180 lb. Generally, structural and propulsion weights increase with the number of rotors. There is only one design mission, so the battery capacity equals the energy (including reserve) needed for that mission. Even high specific-energy batteries are heavy, so all-electric propulsion produces a heavier aircraft than turboshaft or hybrid or turbo-electric propulsion. The high cruise efficiency of the lift+cruise type reduces the battery weight compared to the quadrotor, but not enough to counter the increase in structure and propulsion weight, so the all-electric lift+cruise aircraft is the heaviest design.

5.1 Quiet Single Main Rotor Helicopter

The Quiet Single Main Rotor helicopter (QSMR) is representative of a state-of-the-art helicopter designed specifically for the UAM mission [8]. In addition to shorter range for UAM applications, several design decisions were made to bias the design toward low noise. The tools in the toolchain have been validated with legacy helicopters [12–16], including some helicopters with the noise reduction technologies employed in this demonstration. Therefore, the predicted size, weight, performance and noise of the QSMR is expected to be quite close to that of a real aircraft designed to these criteria and with the assumed level of technology. The relative predictions of the other vehicles can therefore be compared to the QSMR, in order to establish a reasonable expectation of the absolute merits and costs.

The impact of rotor noise on community acceptance of helicopters was recognised early, so there have been five decades of work on reducing noise. From the beginning, much of the focus was on the design variables of tip speed and tail rotor size. Based on demonstrated technology, the QSMR concept vehicle uses a turboshaft engine with a sound-absorbing installation (accounted for in weight of engine installation), and the NOTAR (NO TAil Rotor) anti-torque system to eliminate tail-rotor noise. The NOTAR system is heavier than a traditional tail rotor, but can reduce the anti-torque contribution to noise to such an extent that the main rotor is by far the dominant noise source. For low main rotor noise, the design has a low disk loading and low tip speed, hence large blade area and a large number of blades. The direct and indirect results of low tip speed include high rotor and transmission weight, which increases the aircraft takeoff weight. Design excursions include turboshaft and electric propulsion. The effects of blade tip droop and higher-harmonic control on the aircraft noise were examined [8].

5.2 Quadrotor

The quadrotor aircraft is intended to represent multirotor-type aircraft, which use collective or rotor speed control for flight control, without cyclic control [6]. One interesting attribute of the designs for the NASA quadrotor concept aircraft is that the rear rotors are mounted higher on the aircraft than the forward rotors. Initial design work with the free wake comprehensive analysis in CAMRAD II led to this design decision, as a significant reduction in power required for cruise was predicted. Subsequent higher fidelity analysis confirmed the beneficial effect, albeit with a different absolute magnitude. Design excursions include turboshaft, hybrid and electric propulsion. The implications of hingeless blades, rpm control and reciprocating engine propulsion were examined for the single-passenger quadrotor [4].

https://doi.org/10.1017/aer.2021.92 Published online by Cambridge University Press

Table 3. Characteristics of UAM concept vehicles [6, 8–9]

Aircraft		QSMR		Side-by-Side		Quadrotor		Lift+Cruise		Tiltwing
Propulsion		Turboshaft	Electric	Turboshaft	Electric	Turboshaft	Electric	Turbo-electric	Electric	Turbo-electric
Payload	lb	1,200	1,200	1,200	1,200	1,200	1,200	1,200	1,200	1,200
Range	nm	75	75	75	75	75	75	75	75	75
Rotor radius	ft	17.7	23.3	10.8	15.9	9.1	13.8	5.0	5.0	3.6
Disk loading	lb/ft^2	4	3.5	5	4	3.5	3	11.6	15.1	20
Tip speed	ft/sec	450	500	450	450	450	450	450	550	550
$L/D_e = WV/P$		5.4	6.0	5.9	7.2	4.9	5.8	8.5	7.9	8.6
V_{br}	kt	100	84	103	89	112	91	81	83	148
Power	hp	2x241	2x272	2x234	2x234	2x294	4x181	8x126 + 821*	8x189 + 838*	8x244
DGW	lb	3,951	5,980	3,665	5,547	3,678	7,221	7,271	9,482	6,584
Empty weight	lb	2,556	4,770	2,294	4,338	2,282	6,012	5,809	8,274	5,130
Structure	lb	1,190	1,616	1,054	1,533	1,033	1853	2,670	2,973	1954
Propulsion	lb	685	804	558	813	567	1,375	1,772	1866	1918
Battery	lb	0	1,502	0	1,150	0	1,742	254	2058	244

*lift motors + cruise motor

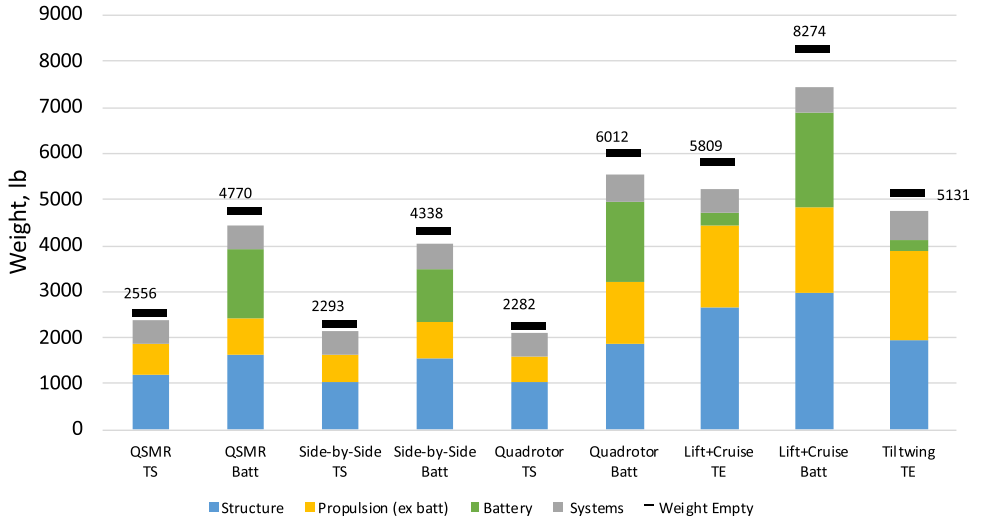

Figure 6. *Structure, propulsion and systems components of empty weight (weight empty = structure + propulsion + systems + vibration control + contingency; TS = turboshaft, TE = turbo-electric).*

5.3 Side-by-side helicopter

The side-by-side helicopter [3, 7] is representative of a high-performance helicopter, which has main rotors that intentionally interact as they physically overlap and intermesh. The side-by-side aircraft has a support crossbar to support the rotors, but this bar does not generate significant lift. The interaction of the main rotors is intended to reduce induced power in forward flight. Design excursions include turboshaft, electric and hybrid propulsion.

5.4 Lift+Cruise aircraft

The Lift+Cruise aircraft [6] is a stopping-rotor thrust- and lift-compound helicopter. There are three distinct flight modes for the aircraft: helicopter mode with the lifting rotors turning, compound mode with lifting and thrusting rotors operating and airplane mode with the lifting rotors stopped and forward thrust is provided by a pusher propeller. In airplane mode, the lifting rotors are stopped with the blade axis pointed along the vehicle longitudinal axis, and therefore nominally aligned with the free stream to minimise drag. Unlike the other concept vehicles, the lift+cruise aircraft can only have two blades on the lifting rotors, so as the rotor speed and solidity changes, no change is allowed in number of blades. The vast majority of lift+cruise aircraft being proposed have fixed rotor pitch and use variable rpm for control. However, to facilitate calculations of aerodynamic interference and noise, investigations can model the aircraft using collective control of the lifting rotors with fixed (identical) rotational speed. Similar to the quadrotor, the lift+cruise aircraft has the rear rotors mounted higher than the front rotors. The performance effects are similar for rotor-rotor interference, but there are now two additional considerations: the influence of the boom for an under-mounted rotor and the interference with the wing. By placing the front rotor under the support boom, a simpler and more compact support can be built. Design excursions include turbo-electric and electric propulsion.

5.5 Tiltwing

The tiltwing vehicle [9] uses a turbo-electric propulsion system to power six proprotors positioned on a tilting main wing and two tilting proprotors positioned on the horizontal tail. All rotors are directly connected to electric motors, with no interconnect shaft. There is a single turboshaft engine connected

https://doi.org/10.1017/aer.2021.92 Published online by Cambridge University Press

to a generator, with a relatively small battery just to enable emergency landing after loss of turboshaft power. Collective control is used, with hover tip speed of 550 ft/sec and cruise tip speed of 300 ft/sec. A tiltwing is of interest for UAM due to its potential to increase cruise speed and efficiency while reducing noise in cruise. The other concept vehicles all have rotors that do not tilt and so either operate in edgewise flight (which limits cruise speed and typically generates more noise than a proprotor in axial flight) or are stopped during cruise (generating drag and weight penalties).

All proprotors are located ahead of the wing leading edge by 3/4 the proprotor radius, in order to reduce the noise caused by wing-rotor interaction; however, this introduces additional challenges in structures (long moment arm) and aerodynamics (the contracted proprotor wake does not yield beneficial aero-propulsive effects along the full span of the wing). The main wing is swept so that the proprotors are longitudinally staggered to prevent cascading proprotor failures. Laterally, the main wing proprotors are placed such that the inboard proprotor is close to the fuselage and the proprotor disks are tangential to one another as viewed from the front. Although this will leave sections of the wing unblown as the slipstream aft of the proprotors contracts, the inflow to the proprotors will be cleaner and the reduced rotor-rotor interaction is expected to reduce noise and increase efficiency. The proprotors at wing tips are positioned such that the shaft axis is coincident with the wing tip to assist in counteracting the wing tip vortex.

6.0 Engineering observations

In examining the vehicles from this series of design investigations, performance targets and recurring technology themes emerged, which may guide investments in research. In addition, results from the various designs support observations about the trade-offs and key design decisions.

These UAM concept aircraft have been used in numerous engineering investigations [27–85], including work on meeting safety requirements, achieving good handling qualities, and reducing noise below helicopter certification levels.

6.1 Battery technology

The most important factor in the feasibility of electrical propulsion systems is the requirement for lightweight, high-power batteries. The baseline designs here assume an installed, usable specific energy of 400 Wh/kg. Current state-of-the-art batteries have installed specific energy of 100–150 Wh/kg. The weight and power variation with range and battery technology are shown in Fig. 7 for an electric side-by-side aircraft. High specific energy enables a useful range with a reasonable aircraft weight and power. Aircraft size does not change the conclusions from these figures, as similar results are obtained for both single-passenger and 15-passenger side-by-side designs [4].

The power capability of batteries is also important. High power is obtained with high current, and current can be characterised by fraction x of the charge capacity C: $I = xC$, with units of 1/hr for x. A maximum burst discharge current of $10C$ to $30C$ (fully discharged in 6 to 2 minutes) is possible for emergency use, but long battery life typically requires currents of $1C$ to $3C$. The discharge current variation with range is shown in Fig. 7 for the electric side-by-side aircraft. The cruise current is less than the hover current for these designs, since cruise speed is fallout (not specified) and the power is sized by the hover condition. The battery capacity is the sum of hover, cruise and reserve requirements:

$$E_{cap} = E_{cruise} + E_{hover} + E_{reserve} \tag{1}$$

Writing cruise power in terms of the aircraft effective lift-to-drag ratio ($P_c = WV/\,(L/D_e)$), the cruise energy is proportional to range:

$$E_{cruise} = (P_c/\eta_c) \times \text{time} = WV \times \text{time}/\,((L/D_e)\,\eta_c) = WR/\,((L/D_e)\,\eta_c) \tag{2}$$

https://doi.org/10.1017/aer.2021.92 Published online by Cambridge University Press

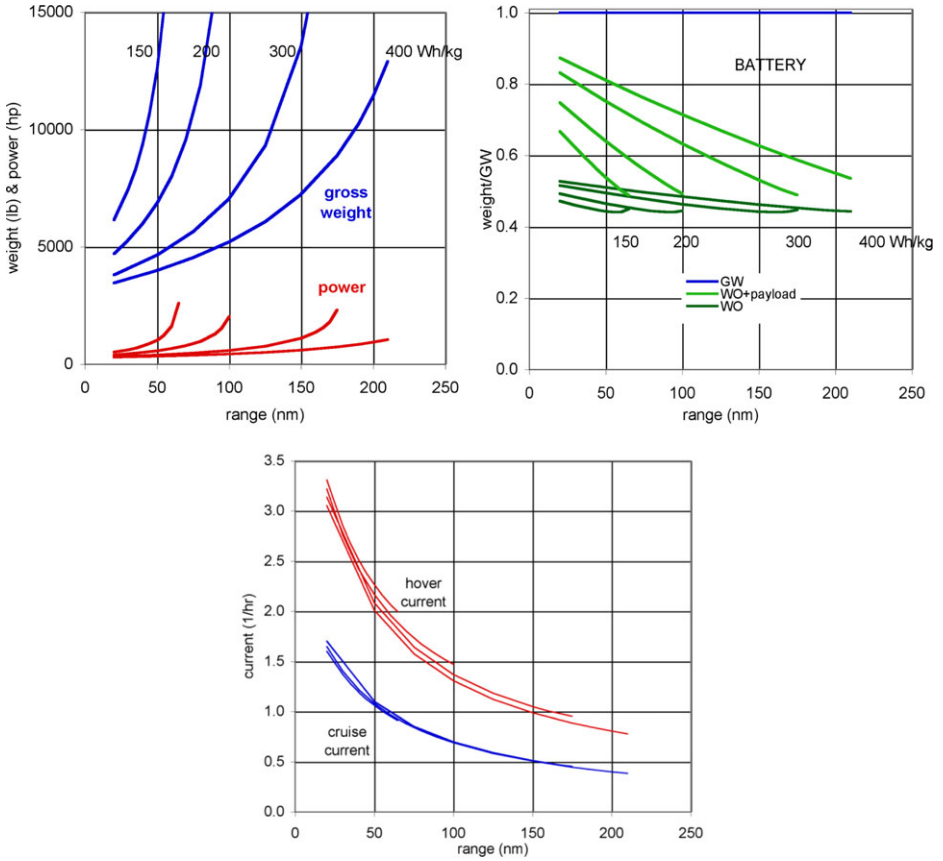

Figure 7. *Electric side-by-side helicopter (six passengers): weight and power variation with range and battery technology; discharge current for battery technology 150–400 Wh/kg (pack).*

where η_c is the propulsion system efficiency in cruise, and the range is $R = V \times$ time. From the charge capacity $C_{cap} = E_{cap}/v$ (for voltage v), and hover current $I = (P_h/v)\ /\eta_h)$ (η_h is the propulsion system efficiency in hover), the hover discharge current is

$$x_{hover} = I/C_{cap} = P_h/\left(\eta_h E_{cap}\right) = \left(W\sqrt{W/2\rho A}/FM\right) / \left(\eta_h E_{cap}\right) \tag{3}$$

with hover power in terms of figure of merit ($P_h = W\sqrt{W/2\rho A}/FM$). Substituting for E_{cap} gives

$$1/x_{hover} = R\frac{\eta_h FM}{\eta_c\ (L/D_e)}/\sqrt{W/2\rho A} + \text{constant} \tag{4}$$

where the constant comes from the hover and reserve energy capacity. Ignoring the constant gives

$$x_{hover} = \sqrt{W/2\rho A}\frac{\eta_c\ (L/D_e)}{\eta_h FM}\frac{1}{R} \tag{5}$$

High hover efficiency (low disk loading and high figure of merit) reduces the current, but short range or high cruise efficiency (L/D_e) reduces the battery capacity required, hence increases the hover current x_{hover}. As illustrated in Fig. 7, this result is independent of battery technology, except as it impacts the range that is achievable by a design. For the side-by-side aircraft, the hover current $x_{hover} < 1C$ if the range is greater than about 160 nm, and $x_{hover} < 2C$ if the range is greater than about 60 nm.

https://doi.org/10.1017/aer.2021.92 Published online by Cambridge University Press

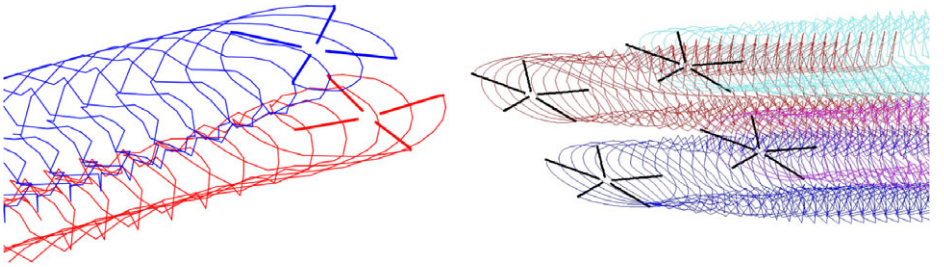

Figure 8. *Wake geometry of side-by-side and quadrotor aircraft at cruise speed.*

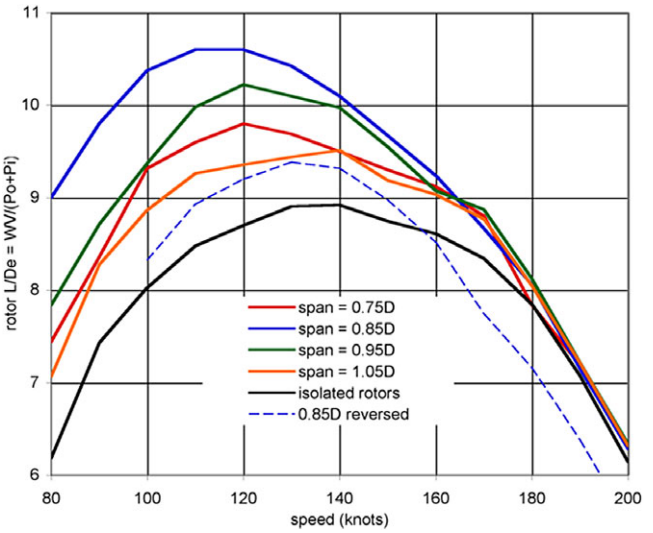

Figure 9. *Rotor cruise efficiency as function of overlap for side-by-side helicopter.*

The conclusion from Fig. 7 is that reasonable hover current requires that the aircraft have a large battery, preferably because of good weight efficiency permitting long range, not because of low cruise efficiency.

6.2 Aircraft aerodynamic efficiency

Electric propulsion is enabled by aerodynamic efficiency of the aircraft, in both hover and cruise. For each design, there is a disk loading that minimises aircraft weight, power, and energy. Small aircraft with edgewise rotors optimise with low disk loading. Rotor-rotor interference must be considered for optimum cruise performance. Interactional aerodynamics impact performance and operation: for tiltwings, wing separation or buffet during conversion must be considered; for tiltrotors, hover download and rotor-tail interactions must be considered. Rotor shape optimisation covers blade twist and taper, tip sweep and droop. Drag minimisation includes hub, rotor support and airframe.

For aircraft with two or more main rotors, interactions between the rotors have a significant impact on performance, vibration, noise and handling qualities. The interactions depend on the arrangement of the rotors. Figure 8 illustrates the wake geometry of the quadrotor and side-by-side aircraft in cruise flight. The overlap of the side-by-side rotors significantly improves the efficiency of cruise flight, because the twin rotors act as a single, large-span wing system. Figure 9 (from [6]) shows the influence of overlap (wing span = 1.0D = rotor diameter means the rotor disks are tangent) on rotor efficiency (rotor $L/D_e = WV/(P_i + P_o)$).

https://doi.org/10.1017/aer.2021.92 Published online by Cambridge University Press

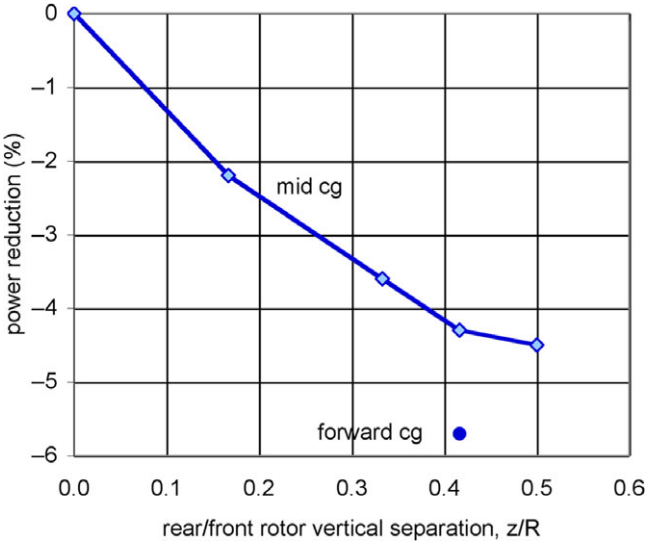

Figure 10. *Influence of elevation of rear rotors on cruise performance of quadrotor.*

Elevating the rear rotors above the front rotors on the quadrotor reduces the cruise power, as shown in Fig. 10 (from [3]), by reducing the interference of the wakes of the front rotors on the rear rotors. Elevating the rear rotors is expected to reduce vibration and noise and improve handling qualities as well. Moving the aircraft center of gravity forward of the mid-point between the rotors, so the front and rear rotors trim closer to the same blade loading C_T/σ at cruise speed, further reduces the power (Fig. 10).

The effects of the rotor-rotor interactions may require vibration and load alleviation systems. The present designs have a weight allocation for vibration control.

6.3 Trim of multi-rotor aircraft

For the quadrotor, both collective and rotor speed control were considered. Figure 11 shows the trim operating conditions of the front and rear rotors for the two control methods. Edgewise rotor flight has reduced induced power (relative hover, for the same lift) due to increased flow through the disk, followed by power increasing with speed as the parasite power increases. The thrust of the rear rotors increases with speed relative the front rotors, for aircraft pitch moment trim. With collective control and fixed rotor speed, the rotor blade loading C_T/σ follows the thrust variation, remaining moderate, while the collective control follows the power variation with speed. With rotor speed control and fixed collective, the rotor rpm follows the power variation with speed, while the rotor C_T/σ increases with speed initially and then decreases (Fig. 11). The increase in C_T/σ might be limited by maximum blade loading, perhaps requiring a smaller design C_T/σ at hover (hence larger blade area).

For the lift+cruise aircraft, Fig. 12 shows the variation with speed of the rotor blade loading C_T/σ and wing lift coefficient. C_L. This design has rigid rotors for hover and low speed lift, using fixed pitch and rotor speed control. The lift rotors are stopped for cruise, with the wing providing all lift. As the induced power decreases with speed, the rotor blade loading C_T/σ increases. As speed decreases, the wing lift coefficient increases, bringing the wing closer to stall. Figure 12 also shows the rotor loading limits due to stall, according to four measures: maximum thrust, change in thrust derivative with collective, four times the profile power and twice the profile power. These hingeless, fixed-pitch rotors operate with large hub roll moments in forward flight (here advance ratio 0.36 and lift offset 0.34 at 90 knots), which increases the loading limits due to stall (a flapping rotor has a steady stall limit of about $C_T/\sigma = 0.12$ at 90 knots). At sufficiently high speeds (here above 90 knots), blade stall encompasses most of the rotor

https://doi.org/10.1017/aer.2021.92 Published online by Cambridge University Press

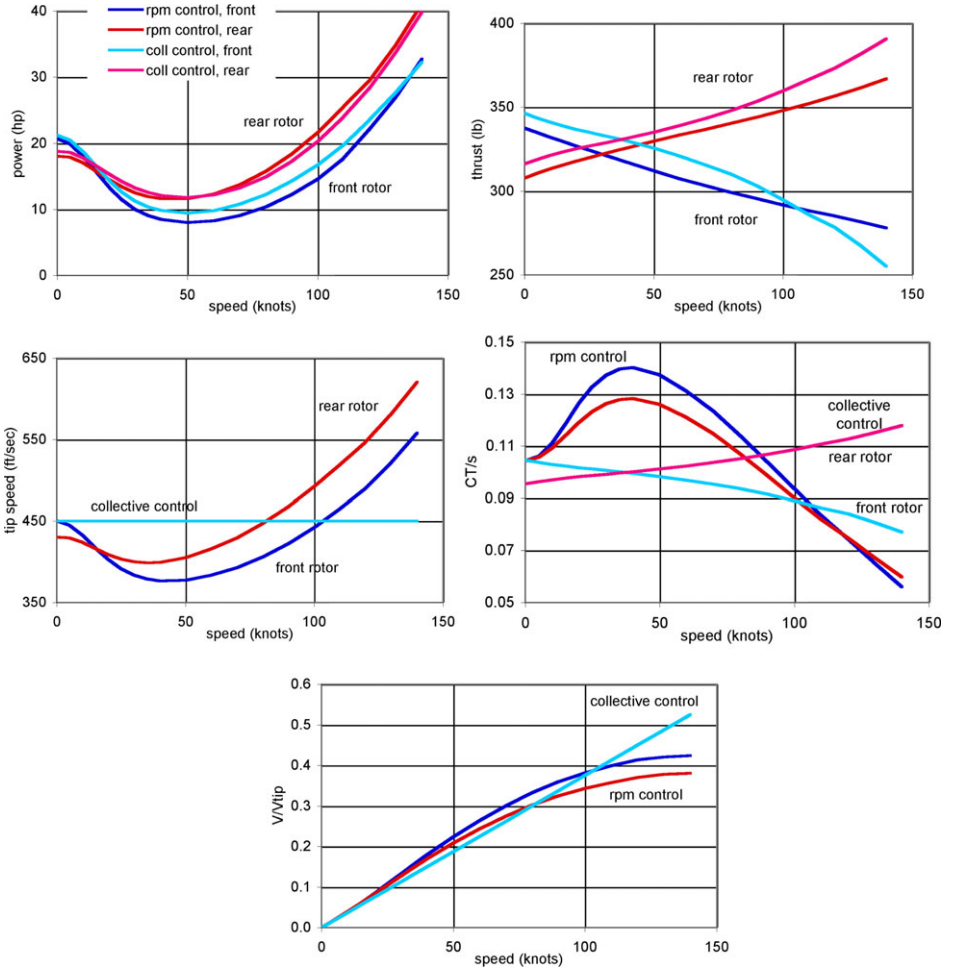

Figure 11. *Electric quadrotor trim as a function of flight speed, for collective control and rotor speed control (with collective control, tip speed and V/V_{tip} are same for front and rear rotors).*

disk, and the C_T/σ limit decreases. The design hover C_T/σ must be low enough and the wing area large enough that transition from rotor-borne to wing-borne flight is possible over a reasonable speed range.

6.4 Rotor/propeller design

Design of the rotor or propeller impacts weight, vibration, and handling qualities. For the quadrotor aircraft, both flapping and hingeless rotors were considered. The flapping rotor had 4% hinge offset, with 45° pitch-flap coupling to minimise flapping relative the shaft. The hingeless or rigid rotor generates higher blade and hub loads, which implies higher rotor weight and vibration-control weight, and the resulting aircraft has 25% larger design gross weight than with flapping rotors.

Figure 13 shows the calculated mean hub moments for the four rotors on the quadrotor aircraft, in level flight and 2g turn. The hub moment is given as lift offset = moment divided by thrust times rotor radius. With no flap hinge and no cyclic pitch, the rotor in edgewise flight operates with increasing lift offset as speed increases. For reference, the design hub moments are shown in Fig. 13 for typical hingeless rotors (Bo-105 level flap stiffness with 10 deg tip-path plane tilt) and lift offset rotors (design load for 200–250 knot aircraft).

https://doi.org/10.1017/aer.2021.92 Published online by Cambridge University Press

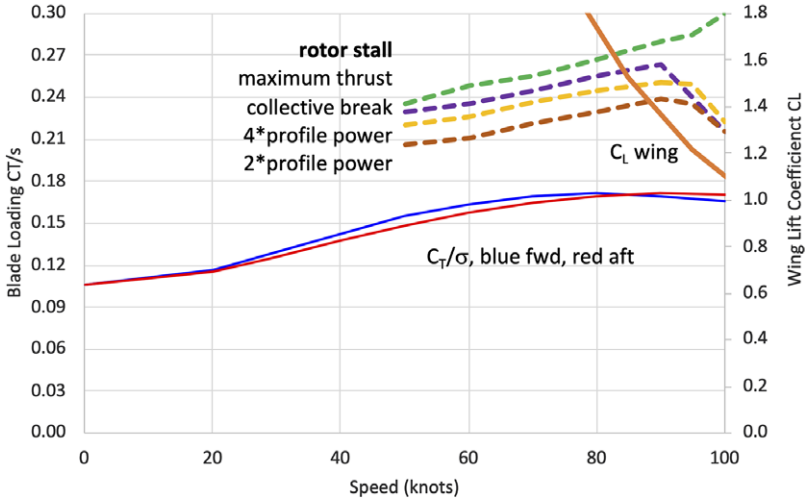

Figure 12. *Lift+cruise aircraft rotor blade loading and wing loading variation with flight speed.*

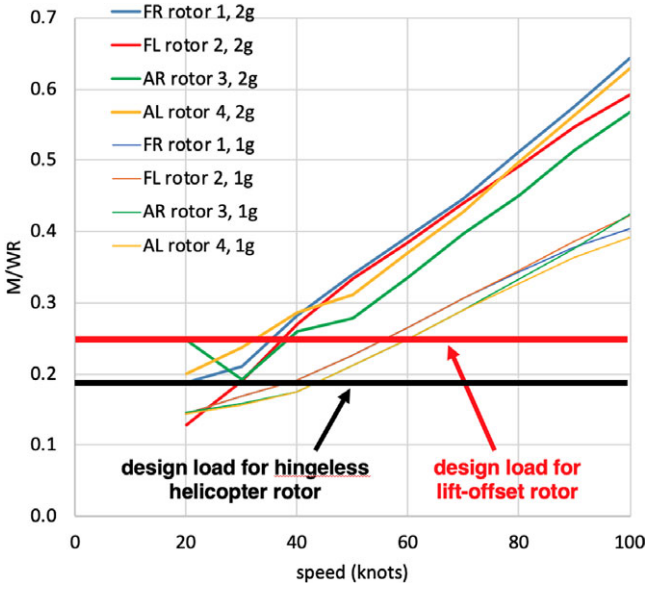

Figure 13. *Quadrotor (fixed pitch, hingeless rotors) mean hub moments in level flight and 2g turn (rotor designation: FR = front right, FL = front left, AR = aft right, AL = aft left); lift offset is M/WR = hub moment divided by thrust times rotor radius.*

All UAM designs will likely require active control of rotorcraft vibration. Fixed-frame active vibration alleviation is common for rotorcraft. In addition, up to 90% reduction of loads and vibration using higher-harmonic control (HHC) or individual blade control (IBC) has been demonstrated through analysis, wind tunnel test and flight test [86]. The UAM designs presented here have technology factors that represent the weight of vibration alleviation systems, excluding HHC or IBC.

6.5 Propulsion system weights

The trend in UAM to explore electric, and in particular distributed electric propulsion (DEP), has introduced the need to model motors, generators, motor controllers, heat exchangers, wiring, and batteries.

https://doi.org/10.1017/aer.2021.92 Published online by Cambridge University Press

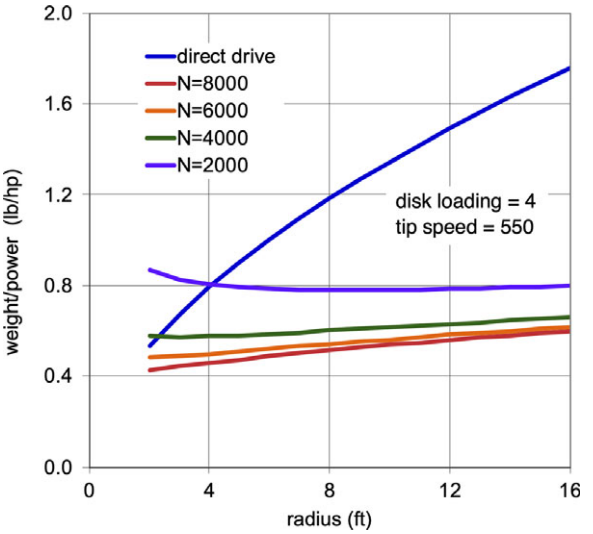

Figure 14. *Motor+transmission weight variation with rotor size and motor speed N (rpm).*

Since 2014, NDARC has had the capability to model electrical propulsion system components, and as more aircraft have been modeled, further empirical and semi-empirical models for elements in the electrical propulsion system have been added to NDARC's built-in capabilities.

Researchers at NASA have used the reference aircraft designs to explore electric architectures including DC, DC/AC, turboelectric and parallel hybrid [35, 51], resulting in extensions to the NPSS software tool. Other research has looked at power transmission wiring design for different material systems [36], finding that the minimisation of vehicle weight may favor lower-density higher-resistance wiring for some architectures. Research into thermal management systems for electric VTOL applications have found that the high power, low mass-flow and small temperature-gradient conditions of eVTOL aircraft in hover present a challenge for cooling design that probably demands a dedicated fan-driven heat exchanger, rather than being able to utilise surface cooling as would be possible for an electric fixed-wing aircraft [53].

Two particular design trades for electric propulsion systems are indicative of the new trades, which may be considered and modeled with the advent of electric propulsion: direct-driven rotors versus motor-plus-gearbox; and fewer large rotors driven by larger motors versus many smaller rotors driven by smaller motors (DEP). The weight of the motor plus transmission of an electric rotorcraft is shown in Fig. 14, as a function of rotor radius for a disk loading of 4 lb/ft^2 and tip speed of 550 ft/sec (typical of the present designs). These weights are calculated using parametric equations for motor and drive system weights [11], with technology factors appropriate for future designs. N is the motor speed (rpm) for cases with a transmission. For direct drive the motor speed equals the rotor speed. These results show that for current and projected future technology, a high-speed (low-torque) motor with an advanced transmission is lighter than direct drive. For direct drive to be the lighter design approach, a light-weight, high-torque motor is required, operating with large mean and oscillatory loads from the rotor.

Figure 15 shows the motor plus transmission weight variation with number of rotors, for a disk loading of 4 lb/ft^2, tip speed of 550 ft/sec, and aircraft weight 5,000 lb. Figure 16 adds the rotor weight to the motor and transmission weight, for design $C_T/\sigma = 0.10$ and flap frequency of 1.25/rev (typical of hingeless helicopter rotors). The rotor weight is calculated using parametric equations [11], which are based on data that includes aircraft weights and rotor diameters corresponding to these designs. Considering just the propulsion system (motor, transmission and rotor), the weight decreases significantly as the number of rotors increases (Fig. 16). Similar results are obtained considering turboshaft engines instead of electric motors, and for a large range of aircraft size. This result is therefore not consistent with the

https://doi.org/10.1017/aer.2021.92 Published online by Cambridge University Press

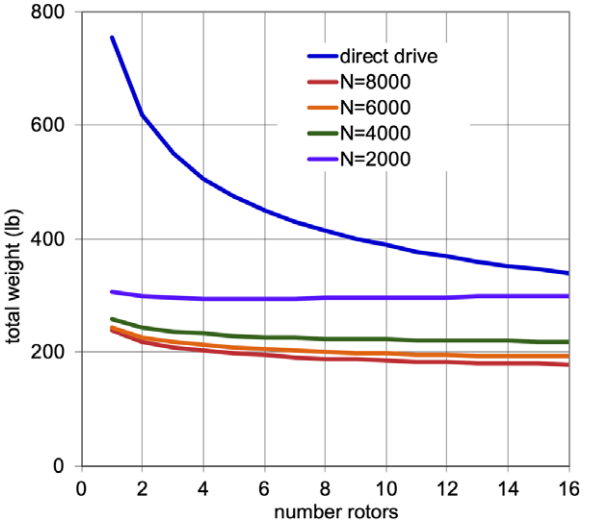

Figure 15. *Motor+transmission weight variation with number of rotors and motor speed N (rpm).*

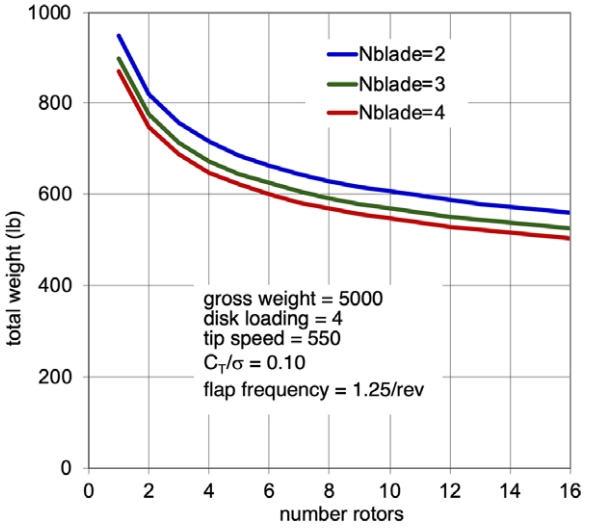

Figure 16. *Motor+transmission+rotor weight variation with number of rotors and number of blades.*

observation that for helicopter designs the single-main-rotor configuration (even with a tail rotor) is preferred to tandem or side-by-side aircraft types. Usually, adding the weight and drag of the structure that supports the rotors changes the optimum solution. Figure 6 shows the empty weights for the concept vehicles designed for the UAM mission. With eight lifting rotors, the lift+cruise type has higher structural weight even though it has good cruise efficiency.

6.6 Structural weights

With the introduction of new aircraft types having very different structural arrangements and different loading conditions, the use of empirical models based on existing helicopters, tiltwings, tiltrotors and fixed wing aircraft is of questionable validity. For the initial design work on the NASA UAM concept vehicles, the existing weight relationships in NDARC were used to model the vehicles, with adjustments

https://doi.org/10.1017/aer.2021.92 Published online by Cambridge University Press

to capture the likely impact of design differences. For instance, the side-by-side aircraft was modeled with a tiltrotor wing for the rotor support beam, using the jump takeoff sizing and preventing the whirl-flutter constraint from becoming active. For the quadrotor rotor support beams, a fixed-weight increment was added to NDARC based on an external calculation of the support beam weight. For the lift+cruise aircraft, the wing was modeled with the NDARC fixed-wing weight equation, and the rotor supports were modeled using the same methodology as applied for the quadrotor.

To address the structural weight uncertainty in the absence of any certified multi-rotor UAM aircraft to be used in development of new weight models, NASA has undertaken to introduce higher-fidelity weight assessment into conceptual design while trying to maintain the flexibility and lack of detailed information that are key features of the conceptual design stage of development. M4 Structures Studio [23] is a tool that interfaces between parametric conceptual geometry in OpenVSP [24] and NASTRAN to rapidly and robustly build finite-element models and maintain the parametric connection to the conceptual design geometry. Using this tool, the structural weights of the initial reference aircraft are predicted to have been in some instances conservatively heavy (side-by-side in [23]) and in other instances optimistically light (lift+cruise in [23]).

As UAM vehicles go through certification and enter operational service, NASA will make an effort to gather as much information as possible about actual weights and driving load conditions, and use this information to calibrate weight models and technology factors.

6.7 Handling qualities

The NASA concept vehicles are being used in explorations of the handling qualities and resulting design implications of these new rotorcraft configurations [40, 47, 60, 75]. Similar investigations are in progress throughout the industry [87–91]. In [75], control models of three vehicles (the quadrotor, an octocopter and the lift+cruise aircraft) were created and compared to determine the effect of rotor number and disk loading on control margin and design. All of these aircraft had electric propulsion with rpm control. In variable rotor speed-controlled vehicles, the propulsion system is directly in the path of the control system, which means the stability and control of the vehicle must be well understood and considered in the process to determine power requirements and the related overall weight of the vehicle.

NDARC was used to size the three, six-passenger vehicles to the same mission. SIMPLI-FLYD [21] was then utilised to generate the bare airframe model. Flight control systems were synthesised using CONDUIT [92] to a common set of handling qualities-oriented guidelines following a multi-objective function optimisation procedure. A model following control system architecture was used, with an integrated electric motor and speed controller. The general optimisation philosophy was to jointly minimise motor usage and crossover frequency, while primarily enforcing closed-loop robust stability margin and performance constraints — disturbance rejection bandwidth (DRB) (and disturbance rejection peak) for the main (heave, roll, pitch and yaw) control loops and minimum steady-state error for the engine speed controller (ESC) loops. Additionally, constraints to ensure minimum eigenvalue damping and crossover frequency were imposed.

All three vehicles met Level 1 handling qualities specifications when the motor current was not constrained. For all three vehicles, the heave and yaw axes demanded more actuator usage (rms current) than the roll and pitch axes. Between heave and yaw, heave was the more demanding because of the dependence of heave on the engine speed controller. The optimised ESC gain and phase margins were large, so the motor control was not a limiting factor. When actuator usage was translated to current margin, torque margin, and power margin, heave was the most demanding axis, followed by yaw, roll, and then pitch for all three vehicles (Fig. 17). the required motor power and torque margins, relative hover, are $P_{max}/P_{hover} = 1.67$ for quadcopter, 2.49 for octocopter and 2.15 for lift+cruise aircraft. The results emphasise the importance of an accurate motor model within the control system architecture.

NASA is also conducting a series of human-in-the-loop (HITL) simulation studies in the NASA Ames Vertical Motion Simulator (VMS). A simulation completed in 2021 investigated the connection

https://doi.org/10.1017/aer.2021.92 Published online by Cambridge University Press

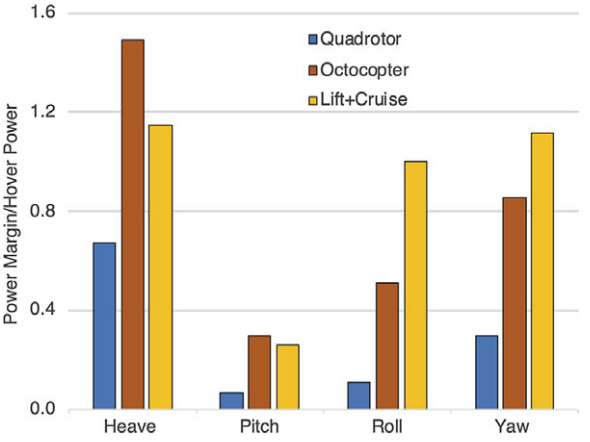

Figure 17. *Power margin (as fraction of hover power) required to achieve level 1 handling qualities [75].*

between engine/motor usage, heave-axis control law design requirements and handling, and ride qualities for all-electric multirotor (quadrotor) architectures using rotor collective or rotor speed (RPM) for control. The studies considered the six-passenger reference quadrotor [6] and a specially designed RPM-controlled variant [75]. The first aircraft was employed as the test control subject, and theoretically configured to be in deep Level 1 handling qualities according to ADS-33. The RPM-controlled variant was configured with varying heave axis pilot response time constants and feedback loop disturbance rejection bandwidths. This approach permitted an examination of tradeoffs in required engine power and handling qualities performance. Low-speed and hover-handling qualities of these configurations, with an Attitude Command-Attitude Hold response type, were evaluated by rotorcraft experimental test pilots in a combination of ADS-33 and specially tailored, UAM-representative mission task elements that emphasised precision over pilot aggressiveness. Preliminary trends frequently showed performance degradation with increased pilot aggressiveness. However, increased time for manoeuvring did not universally correlate with an ability to be more precise. Also, to gain initial insight into UAM passenger susceptibility to motion sickness during flight under smooth (collective control with high-disturbance rejection bandwidth) and moderately rough (RPM control with medium-disturbance rejection bandwidth) flight conditions, a second, complementary study was conducted in the VMS using passenger test subjects. Each participant took two brief (approximately 10 minute) prerecorded simulated quadrotor flights that took off, cruised at an altitude of about 500 ft and then landed at the same San Francisco vertiport. Preliminary findings suggest statistically significant increases in motion sickness symptoms reported, with positive correlation with individual predisposition to motion sickness, for flight under RPM control (medium-disturbance rejection bandwidth) compared to preflight baselines.

6.8 Safety and airworthiness

Airworthiness approval means a document, issued by the FAA for an aircraft, which certifies that the aircraft conforms to its approved design and is in a condition for safe operation (14 CFR 21.1(b)(2)). While certification requirements and procedures for air taxi aircraft may be debated, negotiated, or even contested, for aeromechanics research the focus is on safe operation. Every innovative aircraft type and non-traditional propulsion system requires an extensive failure mode, effects and criticality analysis (FMECA). Important for air taxi aircraft are crashworthiness and the consequences of propulsion system failure. Crashworthiness requirements affect design of airframe structure, landing gear, and passenger accommodation and restraint. Propulsion system failures must be considered in detail. In particular, single as well as complete engine failure must be considered, with requirements for control and methods

https://doi.org/10.1017/aer.2021.92 Published online by Cambridge University Press

for safe landing. In the concept vehicles, degraded weather operation, propulsion system failures and crashworthiness have been assumed to be requirements, and technology factors representing these design considerations have been applied.

6.9 Reliability and safety assessments

NASA commissioned several investigations to contrast major design differences of UAM aircraft and explore the safety and reliability implications from the perspective of vehicle design, propulsion architecture and flight dynamics and control [32, 68–70, 84–85]. The industry is pursuing the issues of UAM aircraft safety [93–95], particularly since EASA's issue of special conditions for VTOL certification and the proposed means of compliance [96–97]. EASA SC-VTOL-01 establishes certification criteria for vertical takeoff and landing vehicles with unique propulsion and control architectures, including distributing the flight controls and electric propulsion elements.

In the initial investigation sponsored by NASA [32, 68], the failure modes and hazards associated with four NASA concept vehicles (1-passenger quadcopter, 6-passenger side-by-side and lift+cruise and 15-passenger tiltwing) were identified and a functional hazard analyses (FHA) and failure modes and effects criticality analyses (FMECA) was performed. A Fault Tree Analysis (FTA) was created for each of the concept vehicles. In addition, conceptual designs of a notional power-train configuration for each of the four concept vehicles were developed to support the reliability and safety analysis for the study. Hazards were identified and the severity of each were categorised in the FHA. Guidelines for reliability targets for both the air vehicle and the operation in the UAM mission were provided. This study provided a methodology for evaluating the safety and reliability of a propulsion architecture.

The recent work sponsored by NASA [70, 84, 85] developed for several of the concept vehicles an all-electric distributed propulsion and flight control (DPFC) architecture that will have no more than 10^{-9} catastrophic failures per flight hour, based on the requirements of EASA SC-VTOL-01. The DPFC architecture included electrical power and distribution system, drive and power system, thermal management system and flight control system. Specific questions regarding number of rotors, control schemes and propulsion type were examined:

A) impact of number of rotors: compare hexacopter and octocopter (electric, rpm control)
B) impact of control schemes: compare rpm control and collective control (hexacopter, electric)
C) impact of propulsion architectures: compare electric, hybrid and turboshaft (quadcopter, collective control, with cross shaft)

The assessments were in terms of the safety level achieved, and aircraft components and features needed to meet the required safety level. Transient stability and control models were developed to help inform vehicle handling characteristics and for system requirements definition. To help characterise safety in all operating environments, transient power requirements were investigated in the presence of atmospheric disturbances representative of an urban canyon environment.

Sizing criteria for power plant components are not currently available for multirotor aircraft; therefore, early stability and control simulations are required to characterise power transients to feed design sizing for both normal and emergency flight conditions. Such simulations show: (a) removing interconnecting shafts results in higher power transients at each motor; (b) rpm control results in higher power transients at each motor, compared to collective control; (c) increasing the number of rotors has a small increase in power transients, but changes to power transients are not as severe as the change to no interconnecting shafts or to rpm control. Table 4 summarises the results for power transients.

DPFC architecture excursions show realistic means to UAM aircraft safety using hybrid-electric or turboshaft power sources: the required safety levels can be achieved using state-of-the-art technology. The turboshaft propulsion architecture is the most reliable of the three considered. Battery networks located at each motor system were required to have at most 10^{-10} failures per flight hour to comply

https://doi.org/10.1017/aer.2021.92 Published online by Cambridge University Press

Table 4. *Required motor power transient capability, P/P_{hover}*

Aircraft Control	Quadrotor Collective	Hexacopter Collective	Hexacopter RPM	Octocopter RPM
Ref. 84				
disturbance rejection (OEI)	2.1	1.4	3.8	3.8
discrete gust		1.75	2.5	2,5
continuous turbulence		2.6	2.5	2.5
Ref. 85				
disturbance rejection		1.35	1.45	1.45
one-engine inoperative		1.4	2.0	2.9

with SC-VTOL-01, which was accomplished by pairing redundant battery packs at each motor, with an impact on aircraft weight. The aircraft with collective control and rpm control exhibit similar reliability levels. Increasing the number of rotors (from 6 to 8) does not inherently increase reliability, due to common cause failures, particularly in the battery system.

All aircraft evaluated likely have paths to comply with the stringent, probabilistic catastrophic failure criteria of EASA SC-VTOL-01. However, the stability and control models showed large power transients that must be addressed. Preliminary system safety assessment results show that future work is needed in single load path structures, high voltage power storage and distribution, and in motor/rotor overspeed protection.

EASA SC-VTOL-01 extends fail-safe and redundancy management design techniques to leverage the potential to segregate failures through unique, multirotor configurations, with stringent design requirements associated with redundancy management and single or multiple load path designs. SC-VTOL-01 requires that a single failure must not have a catastrophic effect upon the aircraft. Certification of conventional rotorcraft configurations imposes similar single failure criteria, except that some exceptions are allowed if the probability of failure is extremely remote. SC-VTOL-01 does not permit catastrophic effects of single failures, regardless of the probability of failure; thus the safety assessment process must demonstrate that all single failures are not catastrophic. The single failure criterion has a potentially large impact on all aircraft intended to be type certificated under SC-VTOL-01. Single-load path structures are of prime concern, being mechanical systems in which redundant load path structures can be difficult to integrate. For example, blade loss, rotor loss or excessive vibrations leading to structural failure are reasonable and conceivable potentially catastrophic failure modes that must be addressed.

6.10 Cost

Purchase cost of aircraft is roughly (to about 20% accuracy) driven by aircraft empty weight, installed power, and complexity, plus the costs of electronic systems. For electric propulsion, the cost of batteries should be explicitly included in the purchase cost estimate. Data are available for maintenance cost of helicopters flying traditional missions, but not for unconventional aircraft types engaged in air taxi operations. A significant component of operating costs is the cost of fuel or energy. If the mission range is small enough so that electric propulsion is feasible, energy costs are generally smaller for the all-electric propulsion configuration, even though the aircraft weight is larger.

A method to estimate the purchase price of rotary wing aircraft was developed by Harris and Scully [98], revised and extended by Scott [99–100]. The method gives the price within 20%, as Price = K (SF), with the size factor

$$\mathrm{SF} = \mathrm{WE}^{0.4638} P^{0.5945} \tag{6}$$

Here WE is the weight empty and P is the installed power; the factor K depends on the aircraft type, and some measures of complexity. The equation Price = K (SF) is applicable to helicopters, tiltrotors,

https://doi.org/10.1017/aer.2021.92 Published online by Cambridge University Press

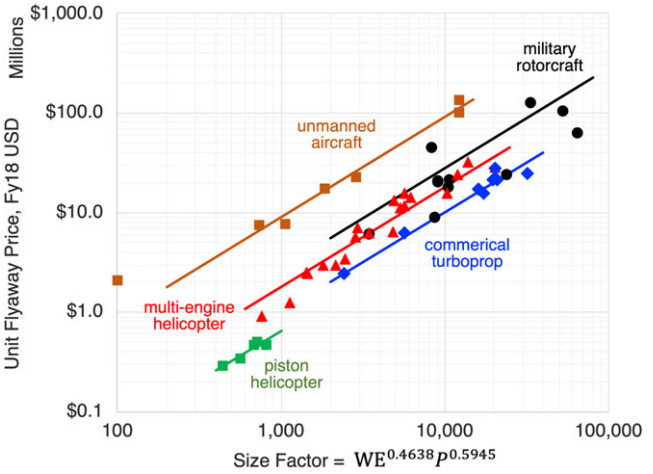

Figure 18. *Unit flyaway price for several classes of rotary wing and propeller aircraft [99].*

general aviation and airlines [85], and to commercial turboprops and unmanned aircraft [86]. The size factor SF appears as a universal scaling parameter for aircraft cost (Fig. 18). The NASA concept vehicles have SF = 1,500 to 6,000, which would imply a unit flyaway cost in the range $3M to $10M following the data in Fig. 18. However, the UAM industry is projecting prices an order of magnitude less than existing rotorcraft and turboprops when high-rate manufacturing is employed and larger numbers of UAM vehicles are produced. There is no data yet to evaluate the factor *K* appropriate for UAM aircraft, but it is reasonable to use this size factor to estimate the relative costs of the concept vehicles.

6.11 Noise and annoyance

The UAM concept vehicles have been designed with low hover tip speed, in anticipation of a significant requirement for noise reduction in the urban environment. Rotor-rotor interactions, such as rear rotors operating in the wake of front rotors, and wake interactions on retreating sides of overlapped side-by-side rotors, will increase blade-vortex interaction noise. Blade shape and spacing can be optimised for low blade-vortex-interaction and high-speed-impulsive noise. Noise metrics and requirements are established by regulation for rotorcraft, but suitability and applicability of these to air taxi operations must be established.

To compare the impact of design variables on the aircraft noise, the noise certification requirements as specified in FAR Part 36, Appendix H, "Noise Requirements for Helicopters," [101] are used. The aircraft is flown over three microphones, at the centerline and 150 m to starboard and port. The operating conditions are sea level pressure, and a temperature of 25°C. Three trajectories are flown: takeoff, flyover and approach. The takeoff profile starts 500 m from the center microphone, 20 m above ground level, and is flown at best rate of climb speed, V_y, and 100% maximum rated power (MRP). The flyover profile is 150 m above ground level, for these aircraft flown at $0.9V_H$, where V_H is the speed at 100% maximum continuous power (MCP). The approach profile has a 6-degree descent angle, flown at V_y, 120 m above ground level at the center microphone. Certification requirements specify the maximum EPNL for these trajectories. NDARC was used to calculate V_y, V_H, and the takeoff climb angle. CAMRAD II calculated the section loading at each condition, and AARON/ANOPP2 calculated the EPNL levels. For each of the reference vehicles, these noise metrics were calculated for a range of design tip speeds.

The aircraft designed to the UAM mission all have relatively high takeoff performance, due to the 900 ft/min climb rate requirement. This results in a higher installed power, so that for the takeoff noise certification condition, the aircraft is both further from the observer than for existing helicopters and the rotor is operating with a quickly convecting wake. These two effects combine to reduce the noise

https://doi.org/10.1017/aer.2021.92 Published online by Cambridge University Press

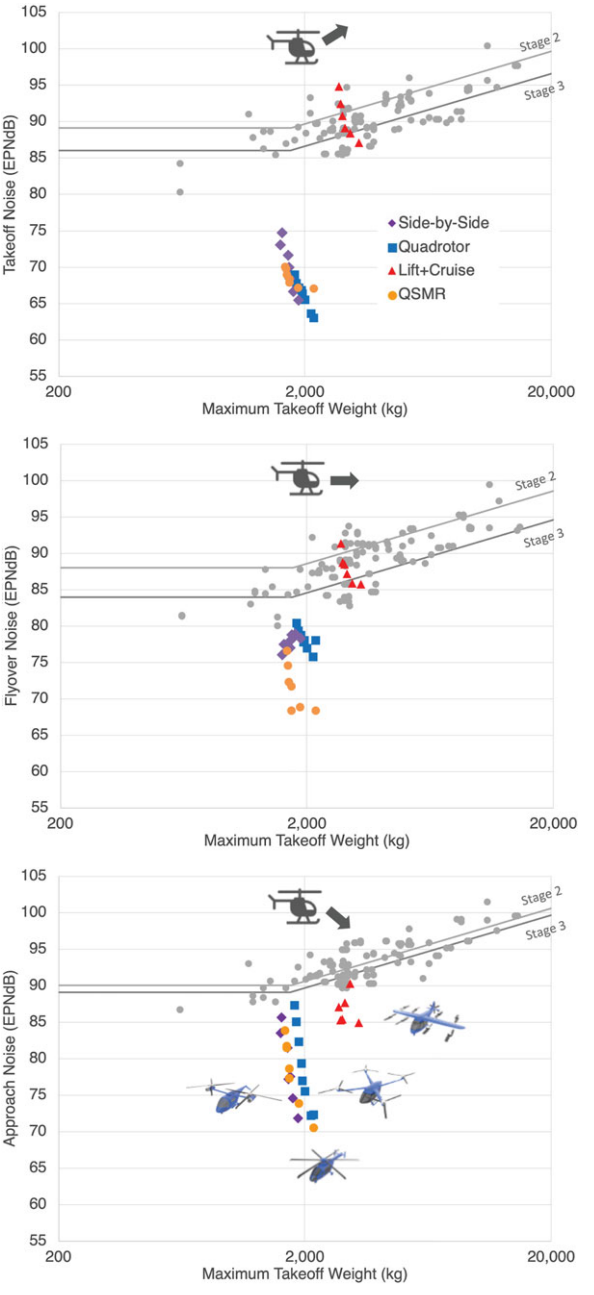

Figure 19. *Noise and max gross weight for the four types of aircraft with varying tip speed compared to existing helicopters (QSMR yellow circle, quadrotor blue square, lift+cruise red triangle, side-by-side purple diamond).*

for the QSMR, quadrotor, and side-by-side by at least 10 EPNdB compared to helicopters of similar weight, as seen in Fig. 19 (takeoff). The colours and markers are consistent in the figures, with QSMR a yellow circle, quadrotor a blue square, lift+cruise a red triangle and side-by-side a purple diamond. The existing helicopter data are shown as grey circles, with grey lines for Stage 2 and Stage 3 limits. The lift+cruise in compound mode trim is the loudest and heaviest of the vehicles, due in large part to the high number of rotors, rotor-rotor interactions and operating at a higher disk loading due to the rotor

https://doi.org/10.1017/aer.2021.92 Published online by Cambridge University Press

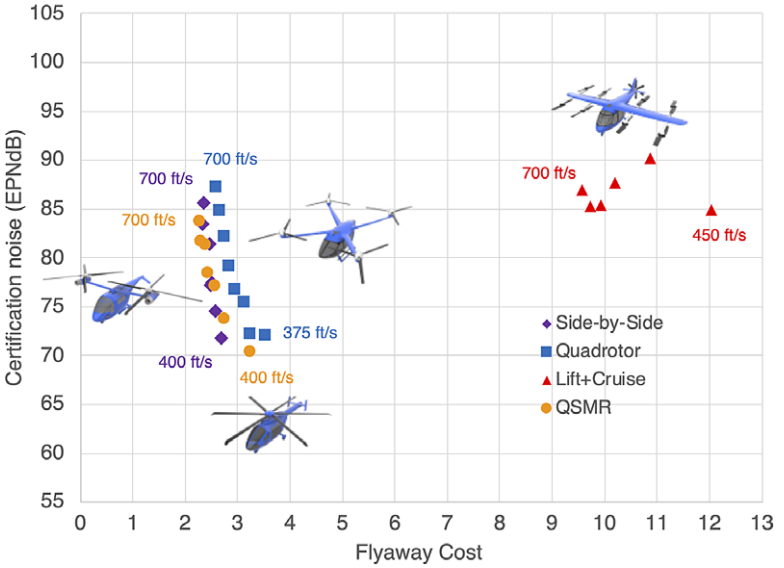

Figure 20. *Approach noise and relative flyaway cost for the four types of aircraft with varying tip speed (QSMR yellow circle, quadrotor blue square, lift+cruise red triangle, side-by-side purple diamond).*

radius being constrained. Flyover results with varying rotor tip speed are shown in Fig. 19 (flyover). For flyover, the QSMR, quadrotor and side-by-side are also in general quieter than existing helicopters, while the lift+cruise is once again similar to existing helicopters. Approach results for varying rotor tip speed are shown in Fig. 19 (approach). Approach noise is close to existing helicopters if the tip speeds are at the higher end of the range of speeds examined, but noise quickly reduces as tip speed goes to the lower end of the range. The lowest tip speed, 375 ft/s for the quadrotor, does not improve the approach noise or the flyover noise compared to the 400 ft/s case.

Vehicle flyaway cost generally increases with rotor tip speed reduction as shown in Fig. 20 (relative costs are shown in this figure). The increase in cost with reducing tip speed is not always accompanied by a reduction in noise, and this trade is likely to be of importance in UAM conceptual design.

7.0 Concluding remarks

NASA is conducting investigations in Advanced Air Mobility (AAM) aircraft and operations. AAM missions are characterised by ranges below 300 nm, including rural and urban operations, passenger carrying as well as cargo delivery. Urban Air Mobility (UAM) is a subset of AAM and is the segment that is projected to have the most economic benefit and be the most difficult to develop. The NASA Revolutionary Vertical Lift Technology project is developing UAM VTOL aircraft designs that can be used to focus and guide research activities in support of aircraft development for emerging aviation markets. These NASA concept vehicles encompass relevant UAM features and technologies, including propulsion architectures, highly efficient yet quiet rotors, and aircraft aerodynamic performance and interactions. The configurations adopted are generic, intentionally different in appearance and design detail from prominent industry arrangements. Already these UAM concept aircraft have been used in numerous engineering investigations, including work on meeting safety requirements, achieving good handling qualities, evaluating vehicle crashworthiness, and reducing noise levels. The NASA concept vehicles for AAM and UAM operations have been described. Focusing on these concept vehicles, observations are made regarding the engineering trade space of Advanced Air Mobility aircraft.

The computational tools available for rotorcraft aeromechanics analysis and design are generally applicable to VTOL AAM aircraft. In particular, the toolchain has been capable of quantitatively trading

https://doi.org/10.1017/aer.2021.92 Published online by Cambridge University Press

several relevant noise reduction technologies and design approaches for aircraft that can perform the Urban Air Mobility mission. The tools are practical for early design applications, in terms of the amount of input required and the computation times.

A high level of battery technology, in particular high energy per weight at the pack level, is a prerequisite for successful development of electric VTOL aircraft. In addition to the direct impact on aircraft size and weight, low-weight batteries also enable the long endurance and range (large battery size) needed to keep hover currents reasonable.

Hingeless rotors or propellers in edgewise forward flight with low tip speed encounter high mean hub moments and blade oscillatory loads, resulting in high-weight rotor designs. Historical data reflecting proven design practices shows that the total propulsion system weight — motors, transmissions and rotors — decreases as the number of rotors increases, a result that holds for all VTOL aircraft sizes, different rotor types (hingeless and hinged), and different propulsion concepts (turboshaft and electric). This trend is, however, reversed when the weight of the structure holding the rotors is included, as illustrated by the concept vehicles.

An assessment of several vehicles (quadrotor, octocopter and lift+cruise configurations) using rpm control showed that Level 1 handling qualities specifications can be met when the motor current is not constrained. When actuator usage was translated to current margin, torque margin, and power margin, heave was the most demanding axis. The control design quantified the significant motor power margins (relative hover power) that must be included in the aircraft sizing. Similar results for transient power capability were found from simulations conducted as part of the reliability and safety assessments.

With AAM designs bringing new solutions to the problems of VTOL flight, there are new measures of success for the first aircraft. Safety and noise are the most important issues, not weight and power, maybe not even cost. The lack of flight experience with multi-rotor configurations utilising electric propulsion makes it imperative to adopt new, rigorous requirements for the response of the aircraft to failures. There are known design choices that will reduce the aircraft noise, and design trades can be made to minimise noise. Work focused on the NASA concept vehicles suggests that designing aircraft for low probability of catastrophic failure and for very low external noise will be possible. The design solutions will require aircraft that are larger and heavier than conventional rotorcraft, with more power and larger energy installed — but the concept vehicle designs imply that such aircraft are still feasible. After safe and quiet aircraft have pioneered the market and introduced passengers to the advantages of AAM, a maturing industry can be expected to return to weight, power, and cost as the classical measures of a good aircraft for the market.

References

[1] Dudley, M.R. Second Annual Transformative Vertical Flight Concepts Workshop. Enabling New Flight Concepts Through Novel Propulsion and Energy Architectures. NASA CR 2016-219141, August 2015.

[2] Antcliff, K.R., Moore, M.D. and Goodrich, K.H. Silicon Valley as an Early Adopter for On-Demand Civil VTOL Operations. AIAA Paper No. 2016-3466, June 2016.

[3] Silva, C., Johnson, W. and Solis, E. Multidisciplinary Conceptual Design for Reduced-Emission Rotorcraft. American Helicopter Society Technical Conference on Aeromechanics Design for Transformative Vertical Flight, San Francisco, CA, January 2018.

[4] Johnson, W., Silva, C. and Solis, E. Concept Vehicles for VTOL Air Taxi Operations. American Helicopter Society Technical Conference on Aeromechanics Design for Transformative Vertical Flight, San Francisco, CA, January 2018.

[5] Patterson, M.D., Antcliff, K.R. and Kohlman, L.W. A Proposed Approach to Studying Urban Air Mobility Missions Including an Initial Exploration of Mission Requirements. American Helicopter Society 74th Annual Forum, Phoenix, AZ, May 2018.

[6] Silva, C., Johnson, W., Antcliff, K.R. and Patterson, M.D. VTOL Urban Air Mobility Concept Vehicles for Technology Development. AIAA Paper No. 2018-3847, June 2018.

[7] Antcliff, K., Whiteside, S., Silva, C. and Kohlman, L. Baseline Assumptions and Future Research Areas for Urban Air Mobility Vehicles, AIAA Paper No. 2019-0528, January 2019.

[8] Johnson, W. A Quiet Helicopter for Air Taxi Operations. Vertical Flight Society Aeromechanics for Advanced Vertical Flight Technical Meeting, San Jose, CA, January 2020.

[9] Whiteside, S.K.S., Pollard, B.P., Antcliff, K.R., Zawodny, N.S., Fei, X., Silva, C. and Medina, G.L. Design of a Tiltwing Concept Vehicle for Urban Air Mobility. NASA TM 20210017971, June 2021.

https://doi.org/10.1017/aer.2021.92 Published online by Cambridge University Press

[10] Silva, C. and Johnson, W. Practical Conceptual Design of Quieter Urban VTOL Aircraft. Vertical Flight Society 77th Annual Forum, May 2021.
[11] Johnson, W. NDARC. NASA Design and Analysis of Rotorcraft. NASA TP 2015-218751, April 2015.
[12] Johnson, W. NDARC — NASA Design and Analysis of Rotorcraft. Validation and Demonstration. American Helicopter Society Specialists' Conference on Aeromechanics, San Francisco, CA, January 2010.
[13] Johnson, W. Technology Drivers in the Development of CAMRAD II. American Helicopter Society Aeromechanics Specialist Meeting, San Francisco, California, January 1994.
[14] Johnson, W. Rotorcraft Aeromechanics Applications of a Comprehensive Analysis. HeliJapan 1998: AHS International Meeting on Rotorcraft Technology and Disaster Relief, Gifu, Japan, April 1998.
[15] Wachspress, D.A., Quackenbush, T.R. and Boschitsch, A.H. First-Principles Free-Vortex Wake Analysis for Helicopters and Tiltrotors. American Helicopter Society 59th Annual Forum, Phoenix, AZ, May 2003.
[16] Lopes, L. and Burley, C. Design of the Next Generation Aircraft Noise Prediction Program: ANOPP2. AIAA Paper No. 2011-2854, June 2011.
[17] Lopes, L.V. Compact Assumption Applied to Monopole Term of Farassat's Formulations. *J Aircr*, 2017, **54**, (5), pp 1649–1663.
[18] Brooks, T.F., Pope, D.S. and Marcolini, M.A. Airfoil Self-Noise and Prediction. NASA RP 1218, July 1989.
[19] Meyn, L.A. Rotorcraft Optimization Tools: Incorporating Rotorcraft Design codes into Multi-Disciplinary Design, Analysis, and Optimization. American Helicopter Society Technical Conference on Aeromechanics Design for Transformative Vertical Flight, San Francisco, CA, January 2018.
[20] Snyder, C.A. and Tong, M.T. "Modeling Turboshaft Engines for the Revolutionary Vertical Lift Technology Project." American Helicopter Society 75th Annual Forum, Philadelphia, PA, May 2019.
[21] Lawrence, B., Theodore, C.R., Johnson, W. and Berger, T. A Handling Qualities Analysis Tool for Rotorcraft Conceptual Designs. *The Aeronautical J*, 2018, **122**, (1252), pp 960–987.
[22] Rohl, P.J., Dorman, P., Cesnik, C.E.S. and Kumar, D. IXGEN — A Modeling Tool for the Preliminary Design of Composite Rotor Blades. American Helicopter Society Future Vertical Lift Aircraft Design Conference, San Francisco, CA, January 2012.
[23] Winter, T., Márquez, J. and Scheneman, B. Development of a Physics-Based Weight (PBWeight) Prediction Tool for Conceptual Design. AIAA Paper No. 2016-4006, June 2016.
[24] Hahn, A. Vehicle Sketch Pad: Parametric Geometry for Conceptual Aircraft Design. AIAA Paper No 2010-657, January 2010.
[25] Derlaga, J.M., Jackson, C.W. and Buning, P.G. Recent Progress in OVERFLOW Convergence Improvements. AIAA Paper No. 2020-1045.
[26] Biedron, R.T., Carlson, J.-R., Derlaga, J.M., Gnoffo, P.A., Hammond, D.P., Jacobson, K.E., Jones, W.T., Kleb, B., Lee-Rausch, E.M., Nielsen, E.J., Park, M.A., Rumsey, C.L., Thomas, J.L., Thompson, K.B., Walden, A.C., Wang, L. and Wood, W.A. FUN3D Manual: 13.7. NASA TM-2020-5010139, November 2020.
[27] Chapman, J.W. Multi-Point Design and Optimization of a Turboshaft Engine for a Tiltwing Turboelectric VTOL Air Taxi. AIAA Paper No. 2019-1948, January 2019.
[28] Jia, Z. and Lee, S. Acoustic Analysis of a Quadrotor eVTOL Design via High-Fidelity Simulations. AIAA Paper No. 2019-2631, May 2019.
[29] Putnam, J. and Littell, J. Evaluation of Impact Energy Attenuators and Composite Material Designs of a UAM VTOL Concept Vehicle. Vertical Flight Society 75th Annual Forum, Philadelphia, PA, May 2019.
[30] Ventura Diaz, P., Johnson, W., Ahmad, J. and Yoon, S. Computational Study of the Side-by-Side Urban Air Taxi Concept. Vertical Flight Society 75th Annual Forum, Philadelphia, PA, May 2019.
[31] André, N. and Hajek, M. Robust Environmental Life Cycle Assessment of Electric VTOL Concepts for Urban Air Mobility. AIAA Paper No. 2019-3473, June 2019.
[32] Darmstadt, P.R., Catanese, R., Beiderman, A., Dones, F., Chen, E., Mistry, M.P., Babie, B., Beckman, M. and Preator, R. Hazards Analysis and Failure Modes and Effects Criticality Analysis (FMECA) of Four Concept Vehicle Propulsion Systems. NASA CR 2019-220217, June 2019.
[33] Ventura Diaz, P., Johnson, W., Ahmad, J. and Yoon, S. The Side-by-Side Urban Air Taxi Concept. AIAA Paper No. 2019-2828, June 2019.
[34] Hendricks, E.S., Falck, R.D., Gray, J.S., Aretskin-Hariton, E.D., Ingraham, D.J., Chapman, J.W., Schnulo, S.L., Chin, J.C., Jasa, J.P. and Bergeson, J.D. Multidisciplinary Optimization of a Turboelectric Tiltwing Urban Air Mobility Aircraft. AIAA Paper No. 2019-3551, June 2019.
[35] Hanlon, P.A., Thomas, G.L., Csank, J.T. and Sadey, D.J. A Tool for Modeling and Analysis of Electrified Aircraft Power Systems. AIAA Paper No. 2019-4403, August 2019.
[36] Aretskin-Hariton, E.D., Schnulo, S., Hendricks, E. and Chapman, J.W. Electrical Cable Design for Urban Air Mobility Aircraft. AIAA Paper No. 2020-0014, January 2020.
[37] Ventura Diaz, P. and Yoon, S. Computational Study of NASA's Quadrotor Urban Air Taxi Concept. AIAA Paper No. 2020-0302, January 2020.
[38] Jia, Z. and Lee, S. Acoustic Analysis of Urban Air Mobility Quadrotor Aircraft. Vertical Flight Society International Powered Lift Conference, San Jose, CA, January 2020.
[39] Li, S.K. and Lee, S. UCD-QuietFly: A New Program to Predict Multi-Rotor eVTOL Broadband Noise. Vertical Flight Society International Powered Lift Conference, San Jose, CA, January 2020.

https://doi.org/10.1017/aer.2021.92 Published online by Cambridge University Press

[40] Malpica, C. and Withrow-Maser, S. Handling Qualities Analysis of Blade Pitch and Rotor Speed Controlled eVTOL Quadrotor Concepts for Urban Air Mobility. Vertical Flight Society International Powered Lift Conference, San Jose, CA, January 2020.
[41] Shastry, A. and Datta, A. Predicting Wake and Structural Loads in RPM Controlled Multirotor Aircraft. Vertical Flight Society Aeromechanics for Advanced Vertical Flight Technical Meeting, San Jose, CA, January 2020.
[42] Hendricks, E.S., Aretskin-Hariton, E.D., Ingraham, D.J., Gray, J.S., Schnulo, S.L., Chin, J.C., Falck, R.D. and Hall, D.L. Multidisciplinary Optimization of an Electric Quadrotor Urban Air Mobility Aircraft. AIAA Paper No. 2020-3176, June 2020.
[43] Archdeacon, J.L., Iwai, N.H. and Feary, M. Aerospace Cognitive Engineering Laboratory (ACELAB) Simulator for Electric Vertical Takeoff and Landing (eVTOL) Research and Development. AIAA Paper No. 2020-3187, June 2020.
[44] Lewicki, D.G. Unmanned Vertical Takeoff and Lift Propulsion Research for Maneuver Flight Control and Improved Endurance and Range. CCDC U.S. Army Research Laboratory, ARL-CR-0849, June 2020.
[45] Winter, T., Robinson, J., Sutton, M., Chua, J., Gamez, A. and Nascenzi, T. Structural Weight Prediction for an Urban Air Mobility Concept. AIAA Paper No. 2020-2653, June 2020.
[46] Sagaga, J.D.W. and Lee, S. CFD Hover Predictions for the Side-by-Side Urban Air Taxi Concept Rotor. AIAA Paper No. 2020-2795, June 2020.
[47] Schuet, S., Malpica, C., Lombaerts, T., Kaneshige, J., Withrow, S., Hardy, G. and Aires, J. A Modeling Approach for Handling Qualities and Controls Safety Analysis for Electric Air Taxi Vehicles. AIAA Paper No. 2020-3188, June 2020.
[48] Lombaerts, T., Kaneshige, J. and Feary, M. Control Concepts for Simplified Vehicle Operations of a Quadrotor eVTOL Vehicle. AIAA Paper No. 2020-3189, June 2020.
[49] Shaw-Lecerf, M.A., Paris, A., Ingram, C.D., Gu, F. and Chung, W.W. Developing Urban Air Mobility Vehicle Models to Support Air Traffic Management Concept Development. AIAA Paper No. 2020-3191, June 2020.
[50] Pradeep, P., Chatterji, G.B., Sridhar, B., Edholm, K.-M., Lauderdale, T.A., Sheth, K., Lai, C.F. and Erzberger, H. Wind-Optimal Trajectories for Multirotor eVTOL Aircraft on UAM Missions. AIAA Paper No. 2020-3271, June 2020.
[51] Thomas, G.L., Chapman, J.W., Alencar, J.F., Hasseeb, H., Sadey, D.J. and Csank, J.T. Multidisciplinary Systems Analysis of a Six Passenger Quadrotor Urban Air Mobility Vehicle Powertrain. AIAA Paper No. 2020-3564, August 2020.
[52] Chin, J.C., Aretskin-Hariton, E.D., Ingraham, D.J., Hall, D.L., Schnulo, S.L., Gray, J.S. and Hendricks, E.S. Battery Evaluation Profiles for X-57 and Future Urban Electric Aircraft. AIAA Paper No. 2020-3567, August 2020.
[53] Chapman, J.W., Hasseeb, H. and Schnulo, S. Thermal Management System Design for Electrified Aircraft Propulsion Concepts. AIAA Paper No. 2020-3571, August 2020.
[54] Jia, Z. and Lee, S. Aeroacoustic Analysis of a Side-by-Side Hybrid VTOL Aircraft. Vertical Flight Society 76th Annual Forum, October 2020.
[55] Niemiec, R., Gandhi, F., Lopez, M.J.S. and Tischler, M.B. System Identification and Handling Qualities Predictions of an eVTOL Urban Air Mobility Aircraft Using Modern Flight Control Methods. Vertical Flight Society 76th Annual Forum, October 2020.
[56] Putnam, J. and Littell, J. Crashworthiness of a Lift plus Cruise eVTOL Vehicle Design within Dynamic Loading Environments. Vertical Flight Society 76th Annual Forum, October 2020.
[57] Scott, R. and Vegh, J.M. Progress Toward a New Conceptual Assessment Tool for Aircraft Cost. Vertical Flight Society 76th Annual Forum, October 2020.
[58] Sirirojvisuth, N., Briceno, S. and Justin, C.Y. A Life-Cycle Economic Study of eVTOL Air Taxi Service in the U.S. North-East Region. Vertical Flight Society 76th Annual Forum, October 2020.
[59] Snyder, C.A. More/All Electric Vertical Take-Off and Landing (VTOL) Vehicle Sensitivities to Propulsion and Power Performance. Vertical Flight Society 76th Annual Forum, October 2020.
[60] Withrow-Maser, S., Malpica, C. and Nagami, K. Multirotor Configuration Trades Informed by Handling Qualities for Urban Air Mobility Application. Vertical Flight Society 76th Annual Forum, October 2020.
[61] Krishnamurthy, S., Rizzi, S.A., Cheng, R., Boyd, D.D., Jr. and Christian, A. Prediction-Based Auralization of a Multirotor Urban Air Mobility Vehicle. AIAA Paper No. 2021-0587, January 2021.
[62] Kratz, J.L. and Culley, D.E. Enhancement of an Electrified Tilt-Wing Propulsion System Using Turbine Electrified Energy Management. AIAA Paper No. 2021-0875, January 2021.
[63] Acheson, M.J., Cook, J. and Gregory, I. Examination of Unified Control approaches Incorporating Generalized Control Allocation. AIAA Paper No. 2021-0999, January 2021.
[64] Gregory, I.M., Acheson, M.J., Bacon, B.J., Britton, T.C., Campbell, N.H., Cook, J.W., Holbrook, J.B., Moerder, D.D., Murphy, P.C., Neogi, N.A., Simmons, B.M., McMinn, J.D. and Buning, P.G. Intelligent Contingency Management for Urban Air Mobility. AIAA Paper No. 2021-1000, January 2021.
[65] Murphy, P.C., Buning, P.G. and Simmons, B.M. Rapid Aero Modeling for Urban Air Mobility Aircraft in Computational Experiments. AIAA Paper No. 2021-1002, January 2021.
[66] Winter, T., Robinson, J., Sutton, M., Chua, J., Gamez, A. and Nascenzi, T. "Conceptual Design Structural Sizing for Urban Air Mobility." AIAA Paper no. 2021-1722, January 2021.
[67] Weitsman, D. and Greenwood, E. Parametric Study of eVTOL Rotor Acoustic Design Trades. AIAA Paper No. 2021-1987, January 2021.
[68] Beiderman, A., Darmstadt, P.R., Dillard, C. and Silva, C. Hazard Analysis Failure Modes, Effects, and Criticality Analysis for NASA Revolutionary Vertical Lift Technology Concept Vehicles. Vertical Flight Society 77th Annual Forum, May 2021.

https://doi.org/10.1017/aer.2021.92 Published online by Cambridge University Press

[69] Darmstadt, P.R., Chen, E., Beiderman, A., Pathak, S., Arkebauer, A., Dillard, C. and Mistry, M.P. Distributed Electric Propulsion and Flight Control Concept to Meet EASA SC-VTOL-01 10^{-9} Catastrophic Failure Criteria. Vertical Flight Society 77th Annual Forum, May 2021.
[70] Darmstadt P.R., Pathak, S. and Mistry, M.P. Distributed Electric Propulsion and Flight Control Concept to Meet EASA SC-VTOL-01 10^{-9} Catastrophic Failure Criteria. Vertical Flight Society 77th Annual Forum, May 2021.
[71] Li, S.K. and Lee, S. Acoustic Analysis of a Quiet Helicopter for Air Taxi Operations. Vertical Flight Society 77th Annual Forum, May 2021.
[72] Littell, J., Putnam, J. and Cooper, M. Simulation of Lift plus Cruise Vehicle Models to Define a Full-Scale Crash Test Campaign. Vertical Flight Society 77th Annual Forum, May 2021.
[73] Sagaga, J. and Lee, S. Acoustic Predictions for the Side-by-Side Air Taxi Rotor in Hover. Vertical Flight Society 77th Annual Forum, May 2021.
[74] Singh, R. and Bagai, A. Considerations for Enabling Extreme Unmanned Aerial Systems Through Advanced Technologies. Vertical Flight Society 77th Annual Forum, May 2021.
[75] Withrow-Maser, S., Malpica, C. and Nagami, K. Impact of Handling Qualities on Motor Sizing for Multirotor Aircraft with Urban Air Mobility Missions. Vertical Flight Society 77th Annual forum, May 2021.
[76] Snyder, S., Zhao, P. and Hovakimyan, N. Adaptive Control for Linear Parameter-Varying Systems with Application to a VTOL Aircraft. *Aerospace Science and Technology*, 2011, 112.
[77] Li, S.K. and Lee, S. Prediction of Urban Air Mobility Multirotor VTOL Broadband Noise Using UCD-QuietFly. *Journal of the American Helicopter Society*, 2021, **66** (3).
[78] Chapman, J.W., Thomas, G.L. and Malone, B.P. Development and Integration of a Thermal Management Simulation for a Quadrotor parallel Hybrid Propulsion System. AIAA Paper No. 2021-3336, August 2021.
[79] Krishnamurthy, S., Aumann, A.R. and Rizzi, S.A. A Synthesis Plugin for Auralization of Rotor Self Noise. AIAA Paper No. 2021-2211, August 2021.
[80] Pacini, B., Yildirim, A., Davoudi, B., Martins, J.R.R.A. and Duraisamy, K. Towards Efficient Aerodynamic and Aeroacoustic Optimization for Urban Air Mobility Vehicle Design. AIAA Paper No. 2021-3026, August 2021.
[81] Pradeep, P., Kulkarni, C.S., Chatterji, G.B. and Lauderdale, T.A. Parametric Study of State of Charge for an Electric Aircraft in Urban Air Mobility. AIAA Paper No. 2021-3181, August 2021.
[82] Simmons, B.M., Buning, P.G. and Murphy, P.C. Full-Envelope Aero-Propulsive Model Identification for Lift+Cruise Aircraft Using Computational Experiments. AIAA Paper 2021-3170, August 2021.
[83] Winter, T., Robinson, J., Gamez, A. and Nascenzi, T. Conceptual Design Structural Sizing Using Simplified Crashworthiness Analysis. AIAA Paper No. 2021-2437, August 2021.
[84] Darmstadt, P.R., Pathak, S., Chen, E., Mistry, M.P., Arkebauer, A., Beiderman, A., Dillard, C., Zierten, D., Beckman, M., Monroe, A., Catanese, R., Greene, T. and Preator, R. Reliability and Safety Assessment of Urban Air Mobility Concept Vehicles. NASA CR 2021.
[85] Justin, C., Patel, S., Bouchard, E.D., Gladin, J., Verberne, J., Li, E., Ozcan, M., Rajaram, D., Mavris, D., D'Arpino, M., Aldemir, T., Rizzoni, G., Türkmen, G.S., Mayo, M. and Bivens, C. Reliability and Safety Assessment of Urban Air Mobility Concept Vehicles. NASA CR 2021.
[86] Johnson, W. *Rotorcraft Aeromechanics*. Cambridge University Press, New York, US, 2013, pp. 740–744.
[87] Walter, A., McKay, M., Niemiec, R., Gandhi, F. and Ivler, C. Handling Qualities Based Assessment of Scalability for Variable-RPM Electric Multi-Rotor Aircraft. Vertical Flight Society 75th Annual Forum, Philadelphia, PA, May 2019.
[88] Klyde, D.H., Schulze, P.C., Mitchell, D.G., Sizoo, D., Schaller, R. and McGuire, R. Mission Task Element Development Process: An Approach to FAA Handling Qualities Certification. AIAA Paper No. 2020-3285, June 2020.
[89] Bahr, M., McKay, M., Niemiec, R. and Gandhi, F. Handling Qualities Assessment of Large Variable-RPM Multi-Rotor Aircraft for Urban Air Mobility. Vertical Flight Society 76th Annual Forum, October 2020.
[90] Theron, J.-P., Horn, J.F., Wachspress, D.A. and Enciu, J. Noinlinear Dynamic Inversion Control for Urban Air Mobility Aircraft with Distributed Electric Propulsion. Vertical Flight Society 76th Annual Forum, October 2020.
[91] Walter, A., McKay, M., Niemiec, R., Gandhi, F. and Ivler, C. Hover Handling Qualities of Fixed-Pitch, Variable-RPM Quadcopters with Increasing Rotor Diameter. Vertical Flight Society 76th Annual Forum, October 2020.
[92] Tischler, M., Colbourne, J., Morel, M., Biezad, D., Levine, W. and Moldoveanu, V. CONDUIT — A New Multidisciplinary Integration Environment for Flight Control Development. NASA Technical Memorandum 112203, June 1997.
[93] Woodham, K.P., Graydon, P.J., Borer, N.K., Papathakis, K.P., Stoia, T. and Balan, C. FUELEAP Model-Based System Safety Analysis. AIAA Paper No. 2018-3362, June 2018.
[94] Bauranov, A. and Rakas, J. Urban Air Mobility and Manned eVTOLs: Safety Implications. DASC, IEEE/AIAA 38th Digital Avionics Systems Conference, San Diego, September 2019.
[95] Bendarkar, M.V., Behere, A., Briceno, S. and Mavris, D.N. A Bayesian Safety Assessment Methodology for Novel Aircraft Architectures and Technologies Using Continuous FHA. AIAA Paper 2019-3123, June 2019.
[96] European Union Aviation Safety Agency. Special Condition for Small-Category VTOL Aircraft, EASA SC-VTOL-01, Issue 1, July 2019.
[97] European Union Aviation Safety Agency. Proposed Means of Compliance with the Special Condition VTOL, EASA MOC SC VTOL, Issue 1, May 2020.
[98] Harris, F.D. and Scully, M.P. Rotorcraft Cost Too Much. *Journal of the American Helicopter Society*, 1998, **43**, (1), pp 3–13.
[99] Scott, R. A Design-Centric Evaluation of Multi-Fidelity Cost Modeling Approaches. Forty-Fourth European Rotorcraft Forum, Delft, The Netherlands, September 2018.

https://doi.org/10.1017/aer.2021.92 Published online by Cambridge University Press

[100] Scott, R. A Perspective on the Affordability Challenges of eVTOL. Challenges of eVTOL, Vertical Flight Society 74th Annual Forum, Phoenix, AZ, May 2018.
[101] United States Government. Part 36 — Noise Standards, Aircraft Type and Airworthiness Certification. Code of Federal Regulations, Title 14, Aeronautics and Space.

Cite this article: Johnson W. and Silva C. (2022). NASA concept vehicles and the engineering of advanced air mobility aircraft. *The Aeronautical Journal*, **126**, 59–91. https://doi.org/10.1017/aer.2021.92